

DTIC FILE COPY

2

AD-A201 863

NAVAL POSTGRADUATE SCHOOL Monterey, California



THESIS

SEA SURFACE TEMPERATURE AND SALINITY
STRUCTURE OF COLD
UPWELLING FILAMENTS NEAR POINT ARENA
AS OBSERVED USING
CONTINUOUS UNDERWAY SAMPLING SYSTEMS

by

Richard L. Snow

June 1988

Thesis Advisor

Steven R. Ramp

Approved for public release; distribution is unlimited.

DTIC
ELECTE
DEC 29 1988
S H D

88 12 28 113

Unclassified

security classification of this page

ADA201863

REPORT DOCUMENTATION PAGE				
1a Report Security Classification Unclassified		1b Restrictive Markings		
2a Security Classification Authority		3 Distribution Availability of Report		
2b Declassification Downgrading Schedule		Approved for public release; distribution is unlimited.		
4 Performing Organization Report Number(s)		5 Monitoring Organization Report Number(s)		
6a Name of Performing Organization Naval Postgraduate School	6b Office Symbol (if applicable) 35	7a Name of Monitoring Organization Naval Postgraduate School		
6c Address (city, state, and ZIP code) Monterey, CA 93943-5000		7b Address (city, state, and ZIP code) Monterey, CA 93943-5000		
8a Name of Funding Sponsoring Organization	8b Office Symbol (if applicable)	9 Procurement Instrument Identification Number		
8c Address (city, state, and ZIP code)		10 Source of Funding Numbers		
		Program Element No	Project No	Task No
		Work Unit Accession No		
11 Title (Include security classification) SEA SURFACE TEMPERATURE AND SALINITY STRUCTURE OF COLD UPWELLING FILAMENTS NEAR POINT ARENA AS OBSERVED USING CONTINUOUS UNDERWAY SAMPLING SYSTEMS				
12 Personal Author(s) Richard L. Snow				
13a Type of Report Master's Thesis	13b Time Covered From To	14 Date of Report (year, month, day) June 1988	15 Page Count 71	
16 Supplementary Notation The views expressed in this thesis are those of the author and do not reflect the official policy or position of the Department of Defense or the U.S. Government.				
17 Cosatl Codes		18 Subject Terms (continue on reverse if necessary and identify by block number)		
Field	Group	Subgroup	California Current System, Filament Mapping, SST, SDAS	
19 Abstract (continue on reverse if necessary and identify by block number)				
<p>Three quasi-synoptic maps of the surface expression of cold filaments off Point Arena, California were made during a pilot program cruise for the Coastal Transition Zone Experiment from 15-28 June 1987. This study provides a description of the sea surface temperature and salinity fields as observed by the continuous underway sampling system installed onboard the R/V POINT SUR.</p> <p>Transects across the survey region revealed the presence of three distinct filaments. Filament A was typically ~ 100 kilometers in width, extended ~ 300 kilometers offshore and was characterized by 12.5-13.0 ° C temperatures and 32.7-33.0 ‰ salinities. It was observed as a persistent feature throughout the survey period. Imbedded within filament A were two smaller features. Filament B was 25-30 kilometers wide and appeared from imagery to have originated from the north near Cape Mendicino. It was characterized by a 12.0 ° C and 32.7 ‰ signature. Filament C was a narrow, cold, more saline core of water originating in the coastal upwelling region near Point Arena. It was typically 15-25 kilometers wide with temperatures from 10.8-11.3 ° C and salinities greater than 33.0 ‰. Its surface signature was transient with a 6-10 day lifetime.</p> <p>All of the observed filaments had boundaries characterized by strong surface temperature gradients ranging from 0.23 to 1.66 °Ckm⁻¹. The gradient at the southern boundary of the filaments was much stronger than the gradient at the northern boundary. Anomalous heating of the sea surface was observed during one transect where the maximum difference between the skin temperature and the two meter temperature was 4.7 ° C. This difference can be accounted for by solar heating of a surface microlayer less than two meters deep.</p>				
20 Distribution Availability of Abstract		21 Abstract Security Classification		
<input checked="" type="checkbox"/> unclassified unlimited <input type="checkbox"/> same as report <input type="checkbox"/> DTIC users		Unclassified		
22a Name of Responsible Individual Steven R. Ramp		22b Telephone (Include Area code) (408) 646-3162	22c Office Symbol 68Ra	

DD FORM 1473,84 MAR

83 APR edition may be used until exhausted
All other editions are obsolete

security classification of this page

Unclassified

Approved for public release; distribution is unlimited.

Sea Surface Temperature and Salinity Structure of Cold
Upwelling Filaments Near Point Arena as Observed Using
Continuous Underway Sampling Systems

by

Richard L. Snow
Lieutenant Commander, United States Navy
B.S., United States Naval Academy, 1976

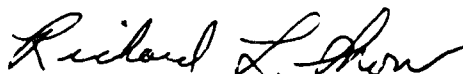
Submitted in partial fulfillment of the
requirements for the degree of

MASTER OF SCIENCE IN METEOROLOGY AND OCEANOGRAPHY

from the


NAVAL POSTGRADUATE SCHOOL
June 1988

Author:



Richard L. Snow

Approved by:



Steven R. Ramp, Thesis Advisor



Roland W. Garwood, Second Reader



Curtis A. Collins, Chairman,
Department of Oceanography



Gordon E. Schacher,
Dean of Science and Engineering

ABSTRACT

Three quasi-synoptic maps of the surface expression of cold filaments off Point Arena, California were made during a pilot program cruise for the Coastal Transition Zone Experiment ⁱⁿ from 15-29 June 1987. This ^{first} study provides a description of the sea surface temperature and salinity fields as observed by the continuous underway sampling system installed onboard the R/V POINT SUR.

Transects across the survey region revealed the presence of three distinct filaments. Filament A was typically ~100 ^{km wide} kilometers in width, extended ~300 kilometers offshore and was characterized by 12.5-13.0 °C temperatures and 32.7-33.0 ‰ salinities. It was observed as a persistent feature throughout the survey period. Imbedded within filament A were two smaller features. Filament B was 25-30 ^{km wide} kilometers wide and appeared from imagery to have originated from the north near Cape Mendicino. It was characterized by a 12.0 °C and 32.7 ‰ signature. Filament C was a narrow, cold, more saline core of water originating in the coastal upwelling region near Point Arena. It was typically 15-25 ^{km wide} kilometers wide with temperatures from 10.8-11.3 °C and salinities greater than 33.0 ‰. Its surface signature was transient with a 6-10 day lifetime.

All of the observed filaments had boundaries characterized by strong surface temperature gradients ranging from 0.23 to 1.66 °C km⁻¹. The gradient at the southern boundary of the filaments was much stronger than the gradient at the northern boundary. Anomalous heating of the sea surface was observed during one transect where the maximum difference between the skin temperature and the two meter temperature was 4.7 °C. This difference can be accounted for by solar heating of a surface microlayer less than two meters deep.



Accession For	
NTIS GRA&I	<input checked="" type="checkbox"/>
DTIC TAB	<input type="checkbox"/>
Unannounced	<input type="checkbox"/>
Justification	
By	
Distribution/	
Availability Codes	
Dist	Avail and/or Special
A-1	

TABLE OF CONTENTS

I. INTRODUCTION	1
II. DATA AND METHODS	3
A. DATA ACQUISITION	3
B. USE OF SATELLITE IMAGERY	4
C. DATA RESOLUTION	6
D. SEA SURFACE TEMPERATURE MEASUREMENT	10
III. RESULTS	15
A. PHASE ONE	15
1. Leg 1KL (Figure 9)	16
2. Leg 1JI (Figure 10)	16
3. Leg 1HG (Figure 11)	16
4. Leg 1EF (Figure 12)	18
5. Leg 1DC (Figure 13)	21
6. Leg 1AB (Figure 15)	21
7. Phase One Summary	22
B. PHASE TWO	25
1. Leg 2IJ (Figure 16)	25
2. Leg 2HG (Figure 17)	26
3. Leg 2EF (Figure 18)	28
4. Leg 2ED (Figure 19)	28
5. Leg 2CD (Figure 20)	28
6. Leg 2CB (Figure 21)	30
7. Leg 2AB (Figure 22)	31
8. Phase Two Summary	33
C. PHASE THREE	35
1. Leg 3BA (Figure 23)	36
2. Leg 3BC (Figure 24)	36
3. Leg 3DC (Figure 25)	36
4. Leg 3EF (Figure 26)	38

5. Phase Three Summary	39
D. SEA SURFACE TEMPERATURE ANOMALY	40
E. HEAT BUDGET CONSIDERATIONS	44
IV. DISCUSSION	51
V. CONCLUSIONS	57
VI. LIST OF REFERENCES	59
VII. INITIAL DISTRIBUTION LIST	61

LIST OF TABLES

Table 1.	VARIABLES MONITORED AND RECORDED BY THE SDAS 3
Table 2.	SIGNIFICANT MEASUREMENTS OF FILAMENT C 35
Table 3.	SKIN AND TWO METER TEMPERATURES 44
Table 4.	HOURLY VALUES OF AIR-SEA INTERACTION VARIABLES	... 47
Table 5.	CALCULATED BULK PARAMETERS 48
Table 6.	CALCULATED AND OBSERVED HEAT FLUX TERMS 50

LIST OF FIGURES

Figure 1.	Pre-cruise AVHRR Imagery From June 10, 1987	5
Figure 2.	Analysis of AVHRR Sea Surface Temperature Field	6
Figure 3.	Phase One Track Superimposed on 16 June AVHRR Infrared Imagery .	7
Figure 4.	Phase Two Track Superimposed on 21 June AVHRR Infrared Imagery .	8
Figure 5.	Phase Three Track Superimposed on 22 June AVHRR Infrared Imagery	9
Figure 6.	Arrangement of Boom Probe Sensor Onboard R/V POINT SUR.	11
Figure 7.	Evolution of Mixed Layer Depth 21-22 June 1987	13
Figure 8.	Boom and Seachest Temperature Comparison 21-22 June 1987	14
Figure 9.	Temperature and Salinity Along Transect 1KL	17
Figure 10.	Temperature and Salinity Along Transect 1JI	18
Figure 11.	Temperature and Salinity Along Transect 1HG	19
Figure 12.	Temperature and Salinity Along Transect 1EF	20
Figure 13.	Temperature and Salinity Along Transect 1DC	22
Figure 14.	Phase One Track Superimposed on 21 June 1987 AVHRR Imagery ...	23
Figure 15.	Temperature and Salinity Along Transect 1AB	24
Figure 16.	Temperature and Salinity Along Transect 2IJ	26
Figure 17.	Temperature and Salinity Along Transect 2HG	27
Figure 18.	Temperature and Salinity Along Transect 2EF	29
Figure 19.	Temperature and Salinity Along Transect 2ED	30
Figure 20.	Temperature and Salinity Along Transect 2CD	31
Figure 21.	Temperature and Salinity Along Transect 2CB	32
Figure 22.	Temperature and Salinity Along Transect 2AB	33
Figure 23.	Temperature and Salinity Along Transect 3BA	37
Figure 24.	Temperature and Salinity Along Transect 3BC	38
Figure 25.	Temperature and Salinity Along Transect 3DC	39
Figure 26.	Temperature and Salinity Along Transect 3EF	40
Figure 27.	00Z NMC Surface Weather Analysis for June 21, 1987	42
Figure 28.	Photograph of Calm, "Patchy" Conditions	43
Figure 29.	Plots of Primary Variables in the Air-Sea Interaction Problem	46
Figure 30.	Superimposed Geostrophic Velocities	53
Figure 31.	Dynamic Height Field Around Filament A	55

ACKNOWLEDGEMENTS

The guidance and patience of my advisor, Dr. Steven R. Ramp, was an important and essential part of this thesis. Paul Jessen provided invaluable computer programming expertise and was always there when I needed him as a sounding board. I also thank the scientists and crew onboard the R/V POINT SUR during the CTZ pilot survey for providing me with an excellent data set.

Finally, I wish to give my wife a lot of credit for putting up with me throughout the entire thesis process.

I. INTRODUCTION

The California Current System (CCS) is a dynamic, energetic system of currents and eddies and varying hydrography. One recurring phenomenon is the appearance of cold filaments. These filaments originate in nearshore waters where active upwelling occurs and extend seaward for hundreds of kilometers. Their presence has been well documented in studies using satellite infrared imagery to locate the thermal signature of the filament.

In early studies, sequences of imagery were used to provide a series of synoptic "snapshots" which could then be used to postulate the processes affecting changes in the observed sea surface temperature fields [Bernstein *et al.*, 1977]. Comparison of *in situ* data along a filament with concurrent imagery [Rienecker *et al.*, 1985] provided the next step in obtaining a clearer picture of cold filaments.

The recent Coastal Ocean Dynamics Experiment (CODE) used imagery to locate a cold filament in the vicinity of the stationary CODE grid. The R/V WECOMA was then detailed to make several hydrographic sections across the filament. The *in situ* data, together with available imagery provided a high resolution picture of the upwelling filament [Kelly, 1985; Flament *et al.*, 1985; Kosro and Huyer, 1986; Huyer and Kosro, 1987].

The next step in improving the knowledge of cold filaments will be through the Coastal Transition Zone Experiment (CTZ). The CTZ is a five year program sponsored by the Office of Naval Research (ONR) as an Accelerated Research Initiative (ARI). The program included a planning stage (1986), a pilot study (1987), extensive field surveys (1988) and an analysis period (1989-90). The ultimate goal of the CTZ is to gather high resolution, multi-source data to help improve the understanding of the dynamics and kinematics of cold filaments and of the associated current structure and biological implications of these features.

From 15-28 June 1987, a pilot study cruise was conducted onboard the R/V POINT SUR. This thesis provides an initial description of the oceanic variables encountered at the sea surface during hydrographic mapping of cold filaments off Point Arena, California. First, the methods of data collection and analysis will be presented followed by a detailed description of the actual observations. Next, a discussion of features unique to individual filaments and comparisons of common characteristics of all the

filaments encountered will be presented. Finally, a summary of survey results along with conclusions and recommendations will conclude the thesis.

II. DATA AND METHODS

A. DATA ACQUISITION

The goal of the pilot cruise was to map any cold filaments which might be present near Point Arena during the survey period using guidance from AVHRR imagery. CTD casts at discreet stations along with continuous current information using an acoustic doppler current profiler (ADCP) to 350 meters provided data on the horizontal and vertical structure of the filaments. XBT's were used when CTD casts could not be made due to inclement weather. The horizontal structure at the sea surface was obtained at higher resolution using a continuous underway sampling system which measured sea surface temperature and salinity. Additionally, satellite tracked drifting buoys were deployed at the beginning and end of the survey. One of these drifters included a special instrumentation package to measure optical and nutrient properties. This drifter was deployed early and was recovered near the end of the cruise. All navigation, meteorological and oceanographic variables listed in Table 1 were monitored and recorded continuously by a SAIL (Serial ASCII Instrumentation Loop) Data Acquisition System (SDAS).

Table 1. VARIABLES MONITORED AND RECORDED BY THE SDAS

1. Latitude	8. Wind Direction
2. Longitude	9. Wind Speed
3. Date	10. Air Temperature
4. Time	11. Dew Point Temperature
5. Sea Surface Temperature (Skin)	12. Relative Humidity
6. Visible Insolation	13. Sea Surface Temperature (2m)
7. Infrared Insolation	14. Conductivity

The heart of the SDAS is an HP series 200 micro-computer which samples connected sensors and peripheral devices, averages the sensor data over a specified time interval, displays selected parameters in real time on a CRT, and records all data on micro-floppy disks. Following the cruise, all data were transferred to mass storage on the IBM 370 mainframe at NPS. Fortran programming to extract the data from mass storage was provided by P. Jessen at NPS. The program DASEDT provided the means to access the data as either time or distance averaged quantities.

B. USE OF SATELLITE IMAGERY.

During the pre-cruise planning stage, AVHRR imagery was used extensively to formulate an initial sampling scheme. Imagery from June 10, 1987 (Figure 1) indicated the presence of a distinct, very cold filament off Point Arena. When available, updates of the filament position from satellite imagery were transmitted directly to R/V POINT SUR from the Scripps Institution of Oceanography via the World Weather Data transmitting station in La Jolla, California. The information was received in the form of a hand analysis of the sea surface temperature field (Figure 2). These updates were useful for making real-time decisions concerning changes to the sampling plan as the filaments evolved. During the cruise, cloud-free imagery was available in the study region on 16, 21 and 22 June.

The pilot cruise consisted of three distinct phases. The tracks for each are superimposed on AVHRR imagery shown in Figures 3, 4 and 5. In each case, the image used was from the satellite pass which was closest to the actual survey time period. In the case of the first and second phases, there is a good fit between the synoptic AVHRR image and the quasi-synoptic survey. The available imagery for the third phase was already nearly three days old. There was also no clear post-cruise imagery available which might have been used to infer previous filament positions. A general description of each phase of the cruise is included below:

- The first phase, from 15-19 June, was to locate and map the root of a filament, characterize the source water feeding the filament, determine the best location to deploy drifting buoys and to map the entire filament by making transects perpendicular to the offshore strike of the flow, continuing seaward until the filament was no longer discernable. The track for this phase is laid out on satellite imagery from 16 June (Figure 3). At the time of the satellite pass, the POINT SUR was near point J. For at least the first half of this phase, the imagery provided a very good representation of actual conditions.
- The second phase, from 20-23 June, began with a return to the source waters to first find a new filament, then commence mapping it as in phase one. The imagery from late in the day on 21 June (Figure 4) came at nearly the midpoint of the track (between points E and F). Unfortunately, the second phase was halted early due to deteriorating weather, but not until after the signature of the filament being mapped had begun to fade significantly.
- The third phase, from 25-28 June, was mainly concerned with the recovery of the previously deployed, specially instrumented drifter. After the recovery, the remaining time was used to resample some of the transects from the second phase to provide a short time history of the filament development. The last partially clear satellite image for the month of June was on 22 June. The phase three track is shown superimposed on this image (Figure 5).

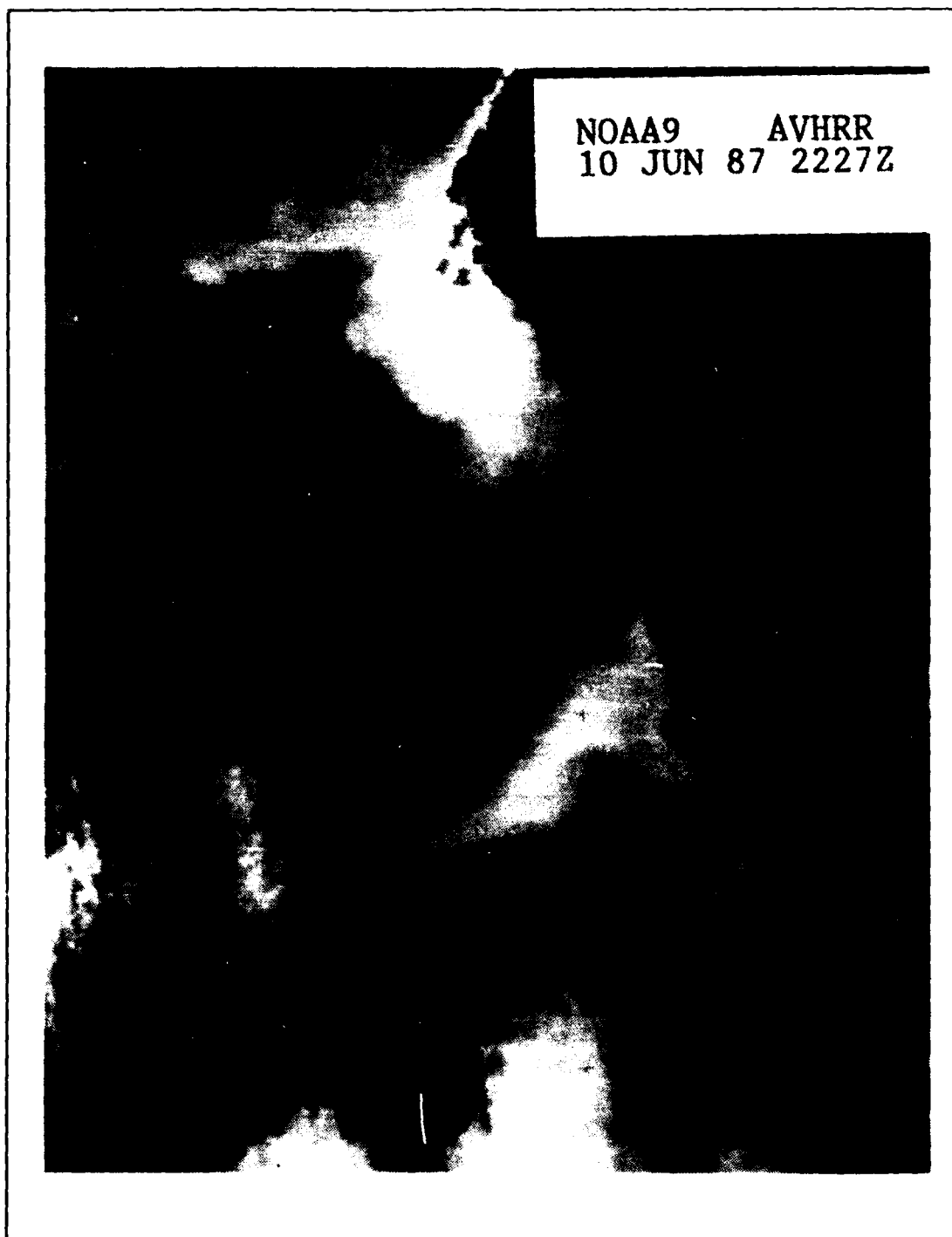


Figure 1. Pre-cruise AVHRR Imagery From June 10, 1987

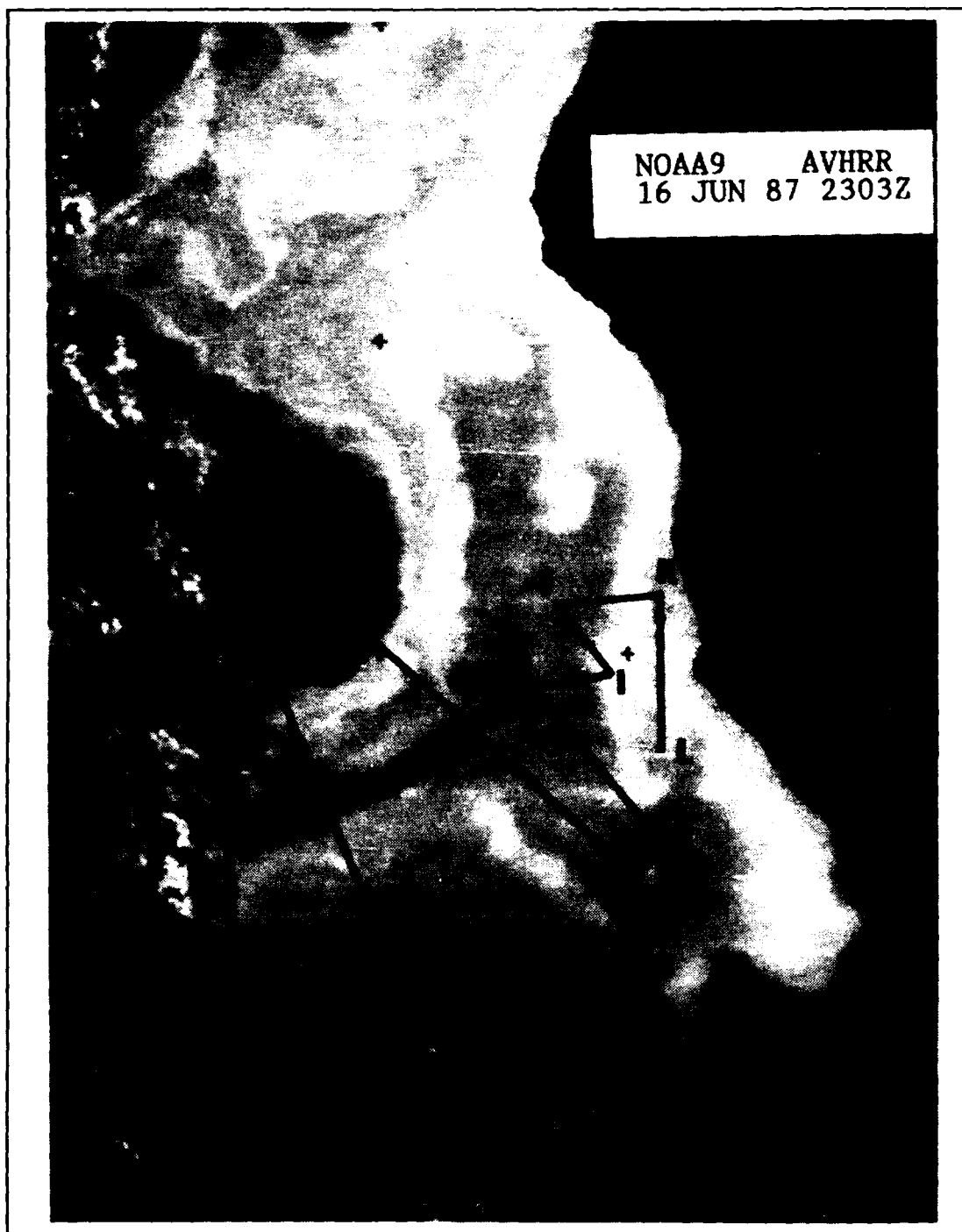


Figure 3. Phase One Track Superimposed on 16 June AVHRR Infrared Imagery

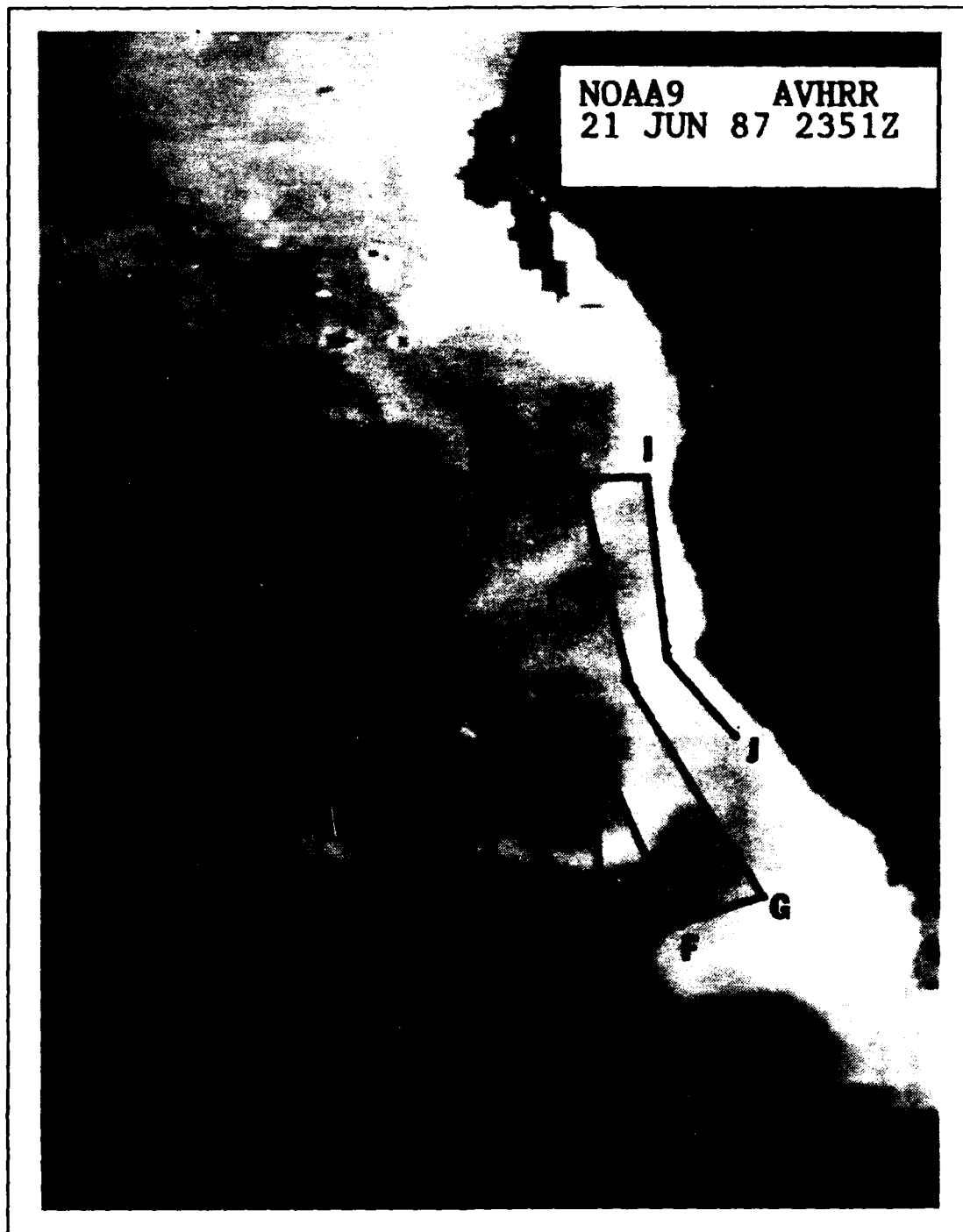


Figure 4. Phase Two Track Superimposed on 21 June AVHRR Infrared Imagery



Figure 5. Phase Three Track Superimposed on 22 June AVHRR Infrared Imagery

The purpose of the continuous underway sampling systems was to resolve the variables of interest (in this case, temperature and salinity) to the finest possible scales. The limits of data resolution were established by two factors: 1) The latitude and longitude were recorded to 0.1 degree accuracy, which corresponds to about 180 meters off Point Arena. 2) The averaging interval for the data being collected was 30 seconds, which at full speed of 6.0 ms^{-1} was also about 180 meters. To obtain a uniform data sample along the cruise track, a spatial "latch filter" was used to accept only points that were greater than the distance "x" from the previous point. The minimum distance "x" that could be used was found to be 360 meters due to the interplay of 1) and 2) above. That is, if the ship, for whatever reason, did not quite travel 180 meters in 30 seconds, then the next point would be accepted, which was 360 meters away from the previous acceptable point. To be sure that no problems were encountered with this data quantizing scheme, the distance "x" was conservatively chosen to be 500 meters which is the effective resolution of the data set. Current AVHRR imagery is able to provide resolution to 1.1 kilometer at nadir, so 500 meter resolution is more than sufficient for satellite shipboard sea surface temperature comparisons.

D. SEA SURFACE TEMPERATURE MEASUREMENT

The R/V POINT SUR was equipped with an underway sampling system consisting of two temperature sensors and a conductivity sensor for determination of salinity. The conductivity sensor and one temperature sensor sampled water from the ship's sea chest, drawn from a depth of approximately two meters below the water surface. The second temperature sensor was designed to sample the very upper few centimeters of the surface layer and will be subsequently referred to as the "skin temperature." A Rosemont platinum resistance thermometer in a heavy brass casing (with only the tip of the thermistor probe exposed) was trailed from a boom perpendicular to the stern of the R/V POINT SUR to provide as near a measurement of actual "skin" temperature as is possible (Figure 6).

The brass casing adds sufficient weight to cause the thermistor probe to remain within four centimeters of the surface when the POINT SUR is underway. During periods when the ship is stopped, the probe sinks to a depth of about one meter. By itself, the response time of the platinum resistance thermometer is estimated to be eight seconds. The brass casing increases the sensor response time by acting as a relatively large thermal mass. The total estimated response time is 60 seconds, thus providing additional assurance against contamination of the skin temperature from exposure to air

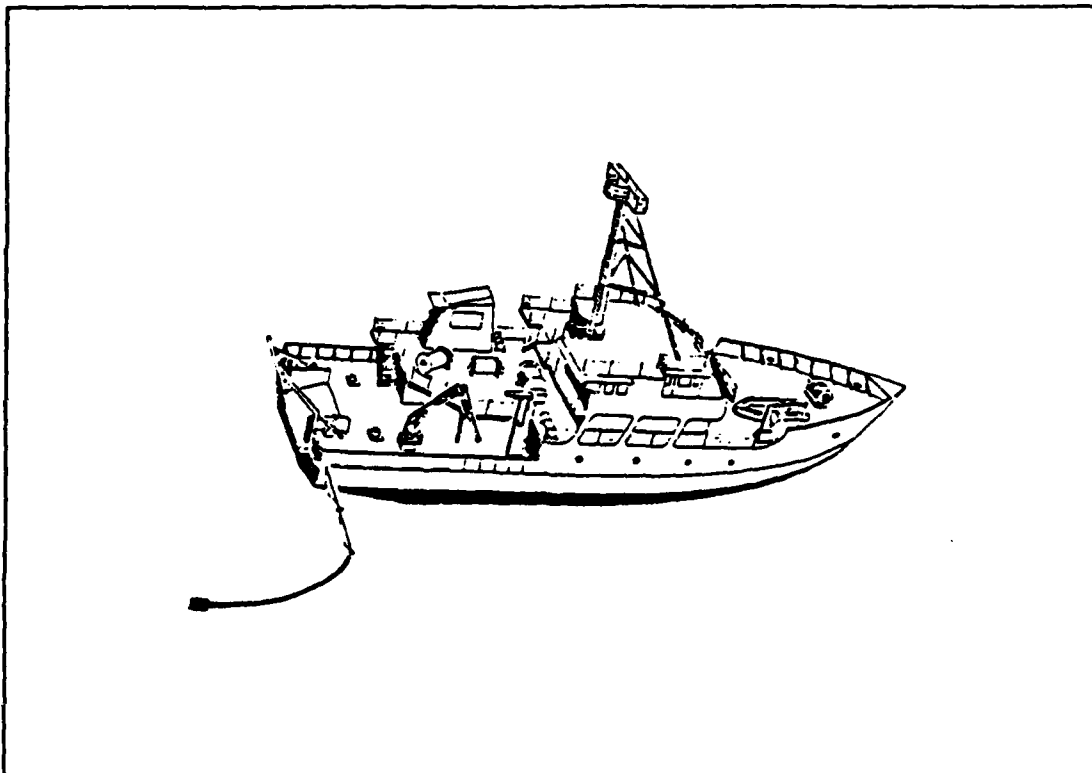


Figure 6. Arrangement of Boom Probe Sensor Onboard R/V POINT SUR.

temperature if it should happen to break the surface. Accuracy of this sensor is estimated to be $\pm .005$ degrees Celsius based on instrument specifications.

The "two meter" temperature is obtained by pumping water from a depth of approximately two meters to an onboard seachest. The temperature is then measured by a SEA-BIRD model SBE-3 oceanographic thermometer which is accurate to $\pm .003$ degrees Celsius. This provides an improvement over previous injection temperature readings which were made near the ship's engines and were invariably contaminated due to the inherent heat source. The response time for this sensor is 72 milliseconds, much faster than the boom probe which had to be a more rugged sensor due to its method of deployment.

The skin and two meter temperatures were expected to be comparable at most times since the surface mixed layer off Point Arena almost always exceeded two meters, as observed during the many CTD and XBT casts throughout the survey. While obtaining a skin temperature cooler than the two meter temperature is possible during periods of

evaporative cooling or when air temperatures are colder than the sea surface creating a negative heat flux, these situations are hydrostatically unstable and are therefore expected to be transient. Throughout the cruise, air temperatures were consistently warmer than the sea surface temperatures with only a few exceptions. Initial analysis of the data indicated that there was a consistent difference between the skin and two meter temperatures, with skin temperature cooler than that at two meters.

First, the question of calibration was addressed. A simple solution would be a constant offset due to differences in calibration methods or calibration times. However, this was not the case. Both instruments were calibrated prior to the cruise on 08 June and following the cruise on 01 July 1987. The boom probe is a resistance measuring thermistor, and the seachest sensor actually measures temperatures. The two were calibrated together in the same controlled water bath. Required corrections for both were recorded for entry into the SDAS onboard R/V POINT SUR. Apparently, the difference noted between the two sensors was real.

The probable source of the offset appears to be the result of heat from the ship transferred through about two meters of piping as the water is pumped from the seachest to the sensor. To determine the value of the offset, data for the period 21-22 June was scrutinized. During this period, wind and sea state increased to the point that CTD casts were impossible and the POINT SUR was forced to seek shelter at Drake's Bay. As seen in Figure 7, the mixed layer depth deepened from near surface to about 40 meters, between 21 June at 1436 and 22 June at 0648.

The presence of vigorous mixing allowed a comparison of the two sensors with a high expectation that their readings should be the same. Figure 8 shows that skin and two meter temperatures were almost identical except for a nearly constant offset. The mean offset for this period was 0.11 degrees Celsius, and the variance was $0.00084^{\circ}\text{C}^2$ (standard deviation of 0.029°C). Another comparison was made between the two meter seachest temperature and the two meter CTD temperature at each station. There was a mean offset between these sensors, with the seachest warmer by 0.124°C and a slightly higher variance of $0.00332^{\circ}\text{C}^2$. The difference in offset and higher variance was not surprising though since the actual depth of the CTD was very hard to determine at the very beginning of a cast. Based on these results, it was assumed that the seachest temperature was high by about 0.11°C , and that the skin temperatures measured by the boom probe were correct. The two meter temperatures were all reduced by 0.11°C to eliminate this offset between the two temperature measurement systems.

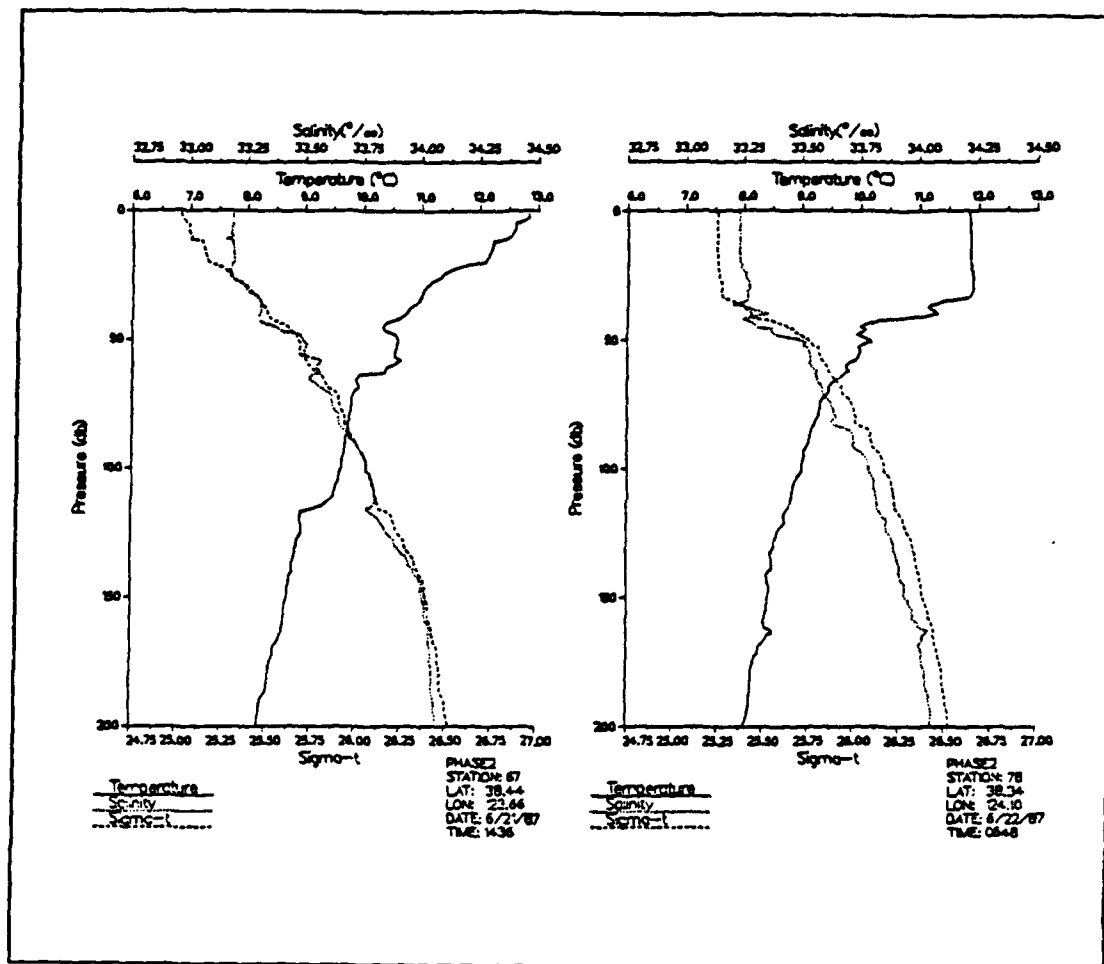


Figure 7. Evolution of Mixed Layer Depth 21-22 June 1987: Showing the effect of the vigorous mixing during the period.

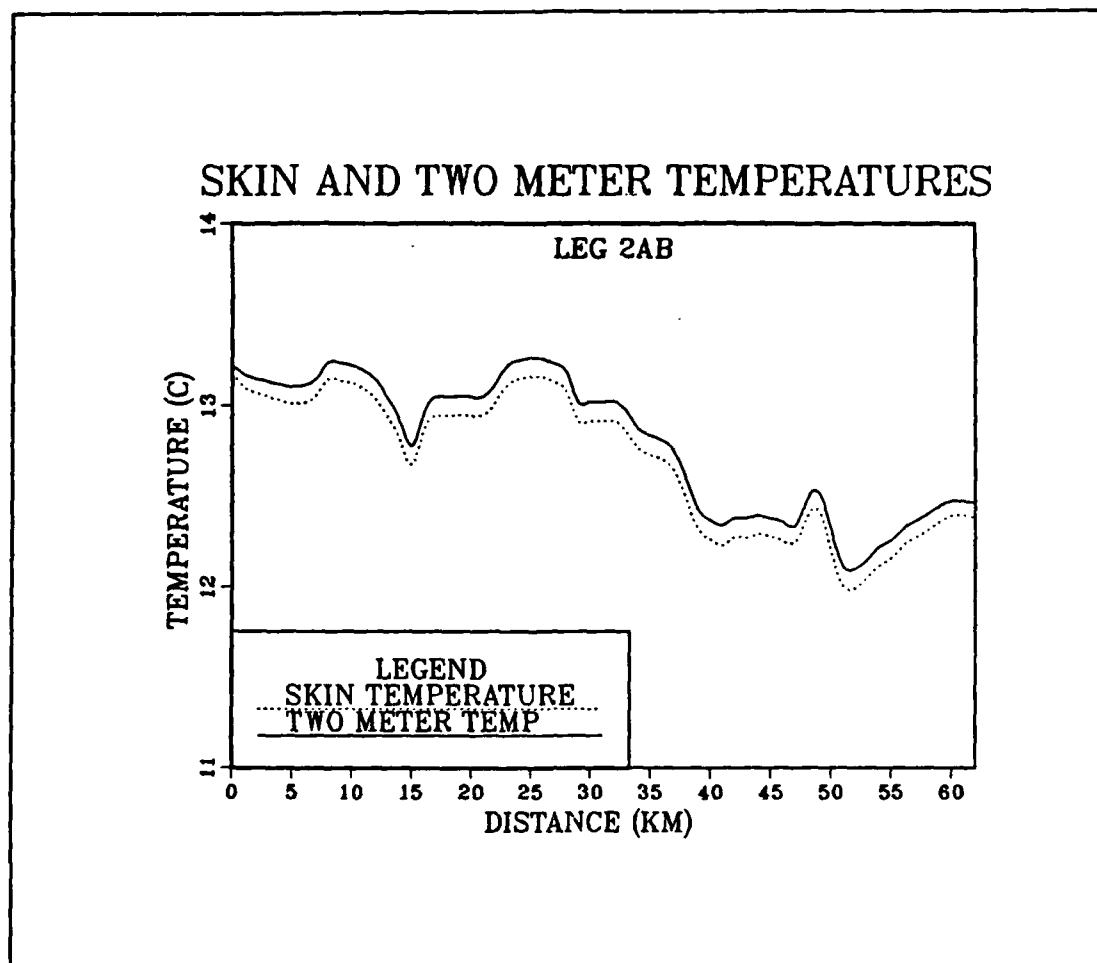


Figure 8. Boom and Seachest Temperature Comparison 21-22 June 1987: Illustrating the near constant offset of 0.11°C between the skin and two meter temperatures during a period of vigorous mixing.

III. RESULTS

The CTZ pilot cruise provided three separate surveys of the surface features of cold filaments off Point Arena. The following sections consist of a complete description of each phase then a comparison of the multiple transects within an individual phase, and finally, an intercomparison between the three phases. The goal is to characterize the surface temperature and salinity signatures of these prominent features as they evolve in space and time.

A. PHASE ONE

Guided by the pre-cruise satellite imagery (Figure 1), the R/V POINT SUR arrived off Point Arena and commenced sampling the filament source waters at 1151 Greenwich mean (Z) time on 16 June 1987 (0451 local time). All times will subsequently be reported in local time which is easier to use in terms of diurnal heating and cooling effects. The starting point is represented on the phase one track laid out on Figure 3 as point L. From this point, mapping of the filament commenced by taking essentially across-filament transects while traversing steadily seaward.

A comparison of Figures 1 and 3 clearly indicated that the cold core imbedded in the broader region of cool water had completely disappeared during the five day lapse in satellite coverage. The only remnant left from Figure 1 was the broad region of cool water hereafter referred to as filament A. Instead of the single, narrow, cold core which was visible in Figure 1 directly off Point Arena, Figure 3 indicated a very complex pattern with filament A broadened and apparently shifted to the south. A second band of cold water, hereafter referred to as filament B, appeared along the northern part of the phase one track (near points D and E) which appears from the imagery to have originated near Cape Mendocino, and been transported southward by an anticyclonic eddy centered near $39^{\circ}30'N$, $125^{\circ}30'W$. Finally, in Figure 3, there was a third cold region between points G and L which ultimately propagated offshore as a narrow, cold core (Figure 4) and is designated as filament C.

Figures 9 through 14 are plots of continuously monitored skin temperature, two meter temperature and salinity along each of the transects of the first phase. Each plot is oriented so that the northern-most point of the transect is to the left and all transects are hereafter referred to by the phase number and the letters along the particular leg with the northern-most letter given first. Start and stop times (which also indicate the

direction the ship was steaming) are noted on the plots. The horizontal scale of each plot is identical so individual features of interest along any of the transects may be readily compared.

1. Leg 1KL (Figure 9)

The source region was characterized by cold ($<12^{\circ}\text{C}$), relatively high salinity ($>33\text{‰}$) water. Since the transect was parallel to the coastal upwelling jet, the presence of a colder core between about the 15 and 55 kilometer points (roughly centered on Point Arena) most probably represented a region of more recently upwelled water. There was also a significant maximum salinity peak ($>33.6\text{‰}$) at about the 18 kilometer point (just north of Point Arena) with a likely similar origin.

Skin and two meter temperatures follow each other closely from the 40-60 kilometer points (approximately time 0800). Between 0 and 40 kilometers, there is a slight separation (0.1°C) indicating the near surface water is warmer than the water just below the surface. The separation can be attributed to the diurnal effect of daytime surface heating due to increased solar insolation.

2. Leg 1JI (Figure 10)

At point J, the surface waters were warmer (about 12.5°C) and less saline ($<33\text{‰}$). At the 15 kilometer point while moving southward towards point I, the temperature began to drop and the salinity began to rise until the same cold, high salinity signature seen during leg 1KL was reached. Daytime heating was apparent for both the skin and two meter temperatures until just before the 15 kilometer point which corresponded to a time of about 1800.

3. Leg 1HG (Figure 11)

Moving further offshore, leg 1HG was the first transect to actually cross filaments A and C at a nearly right angle to the offshore strike. The surface water characteristics at point H were nearly identical to those noted at point J (i.e., not oceanic) but the temperature was not as cold as the temperature of the more recently upwelled water closer to shore. Proceeding towards point G, the surface temperatures remained nearly constant at about 12.5°C until the 30 kilometer point where there was a decrease of $0.30^{\circ}\text{Ckm}^{-1}$ over the next 15 kilometers until a minimum temperature of about 11°C was reached. The cold core of filament C continued to the 55 kilometer point. Then there was a sharp rise of $0.98^{\circ}\text{Ckm}^{-1}$ at the southern boundary of the filament.

Salinity increased gradually along the entire transect with no significant peak. In the vicinity of the cold core, the salinity was slightly greater than 33‰ and was similar

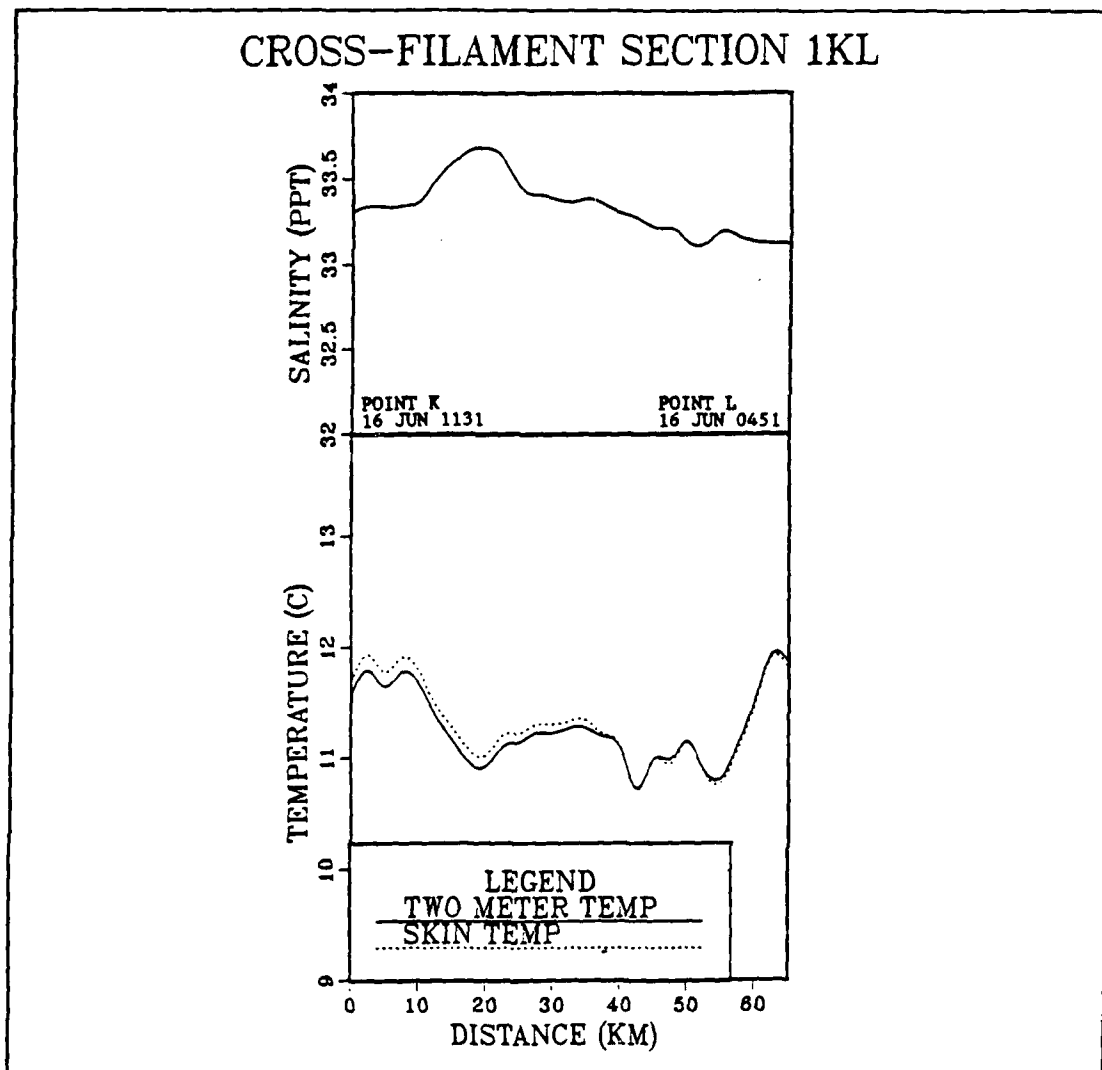


Figure 9. Temperature and Salinity Along Transect 1KL

to that measured at points I and L, which implies that the cold core centered at the 50 kilometer point is an offshore extension of the source water, *i.e.* the beginning of a new cold filament. This interpretation agrees with the impression one gets from examining the satellite imagery (Figure 3). The width of filament C varied between 25 kilometers (measured at the 12°C isoline) and 12 kilometers (measured at the 11°C isoline).

The transect began at about 0100 on 17 June and reached point G at approximately 0730. As expected, in the absence of daytime insolation, there was no indication of differential heating in the skin temperatures (the skin and two meter temperatures

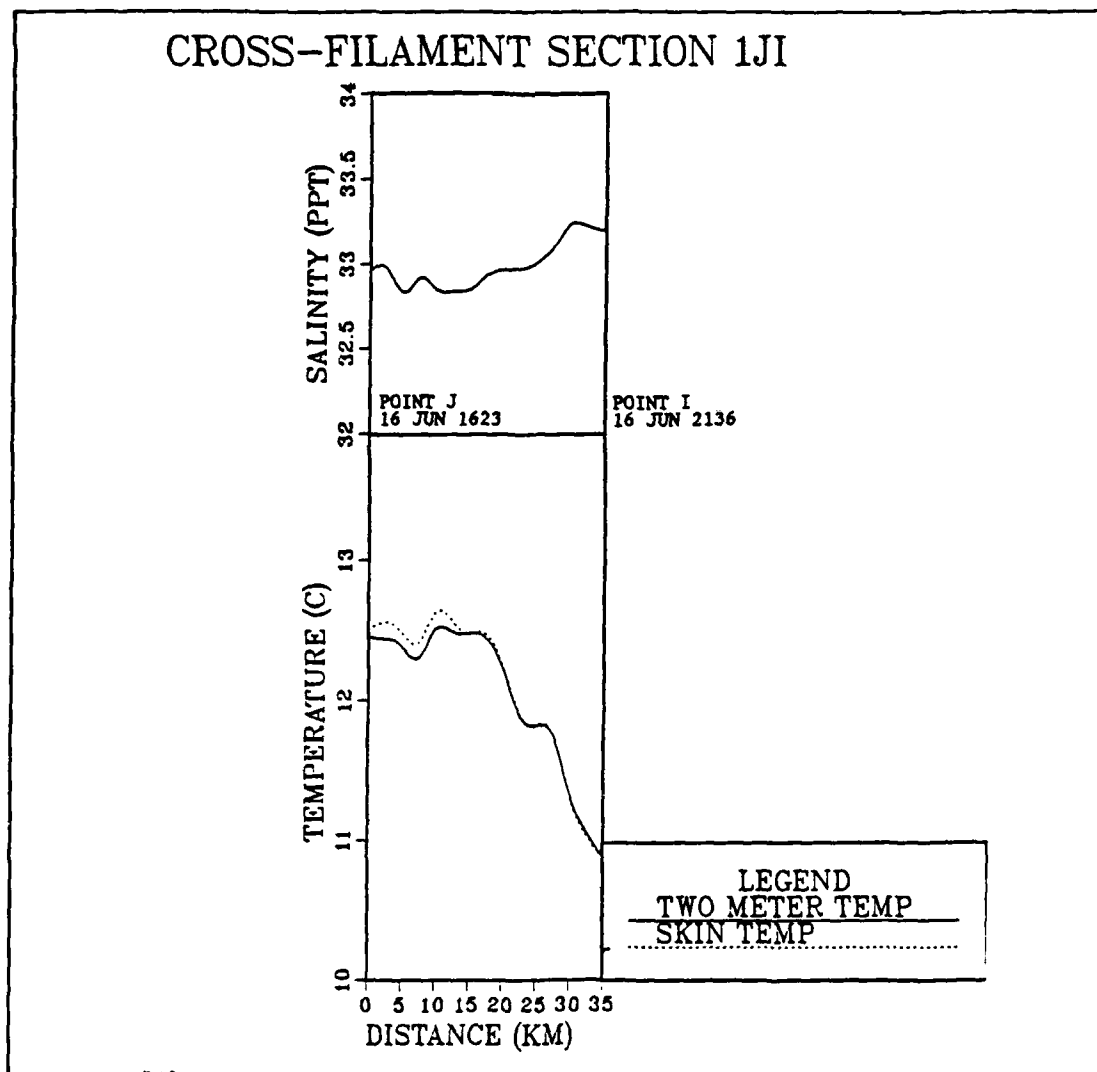


Figure 10. Temperature and Salinity Along Transect 1JI

agreed exactly). Between points G and F there were no temperatures observed for approximately 10 hours while surface drifting bouys were deployed in the core of the cold filament discovered during leg 1HG.

4. Leg 1EF (Figure 12)

The transect between points E and F began at about 1830 on 17 June and concluded at 1219 on the 18th. The cold core located between the 105 and 120 kilometer points was identified as being continuous with filament C observed in leg 1HG. The salinity signature was nearly the same, and the increase in minimum temperature was

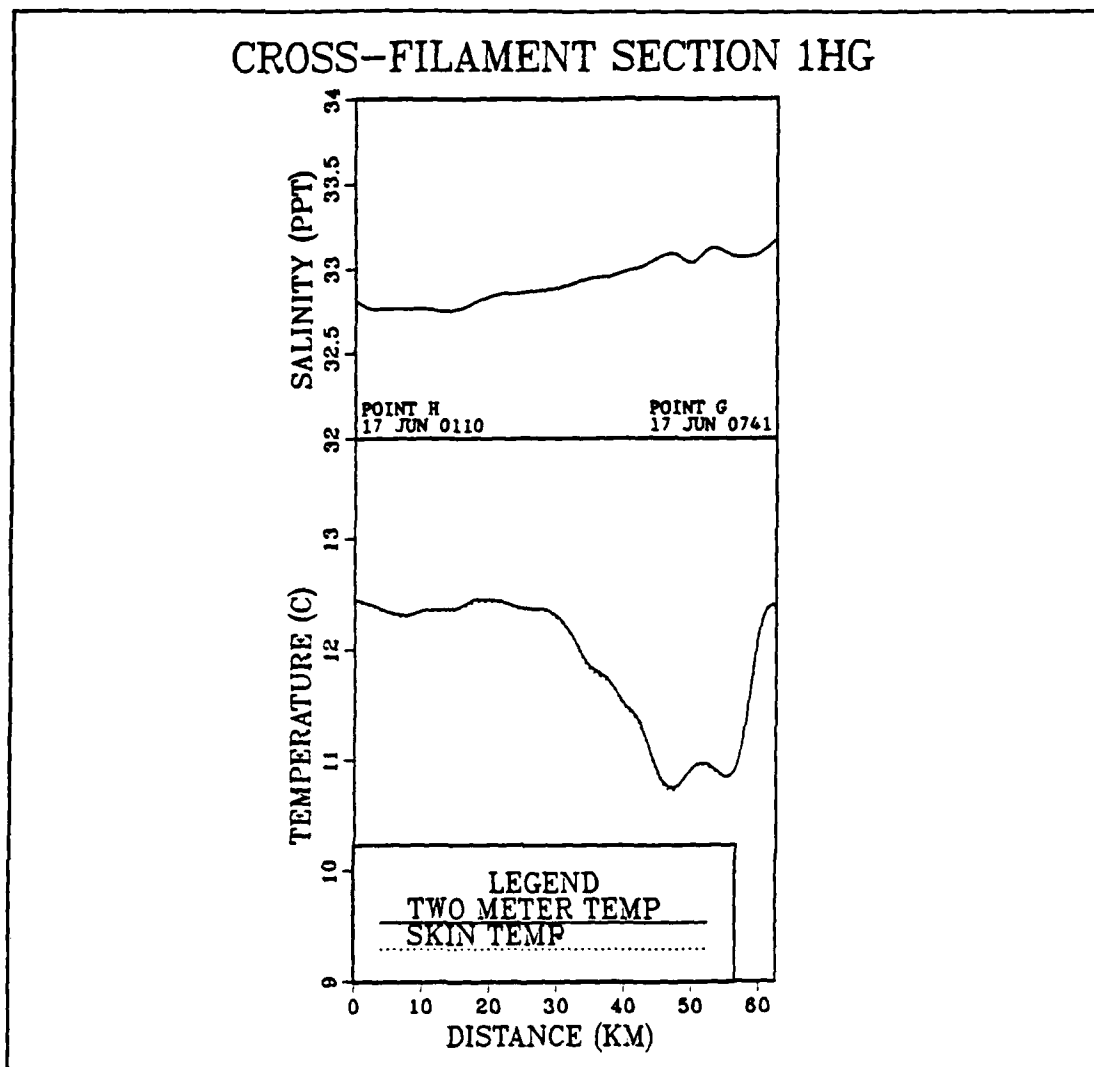


Figure 11. Temperature and Salinity Along Transect 1HG

explainable by possible daytime heating during the period when drifters were being deployed or possibly due to its being the more seaward extension of the filament subjected to additional mixing. The shape of the filament was similar, but the observed minimum temperatures were about one half degree warmer overall. The temperature gradient at the north wall was $0.25^{\circ}\text{Ckm}^{-1}$ while the south wall was much sharper at $1.15^{\circ}\text{Ckm}^{-1}$. The horizontal dimensions of filament C were 12 kilometers measured at 12°C and 18 kilometers measured at 12.5°C , about half the width observed during leg 1HG.

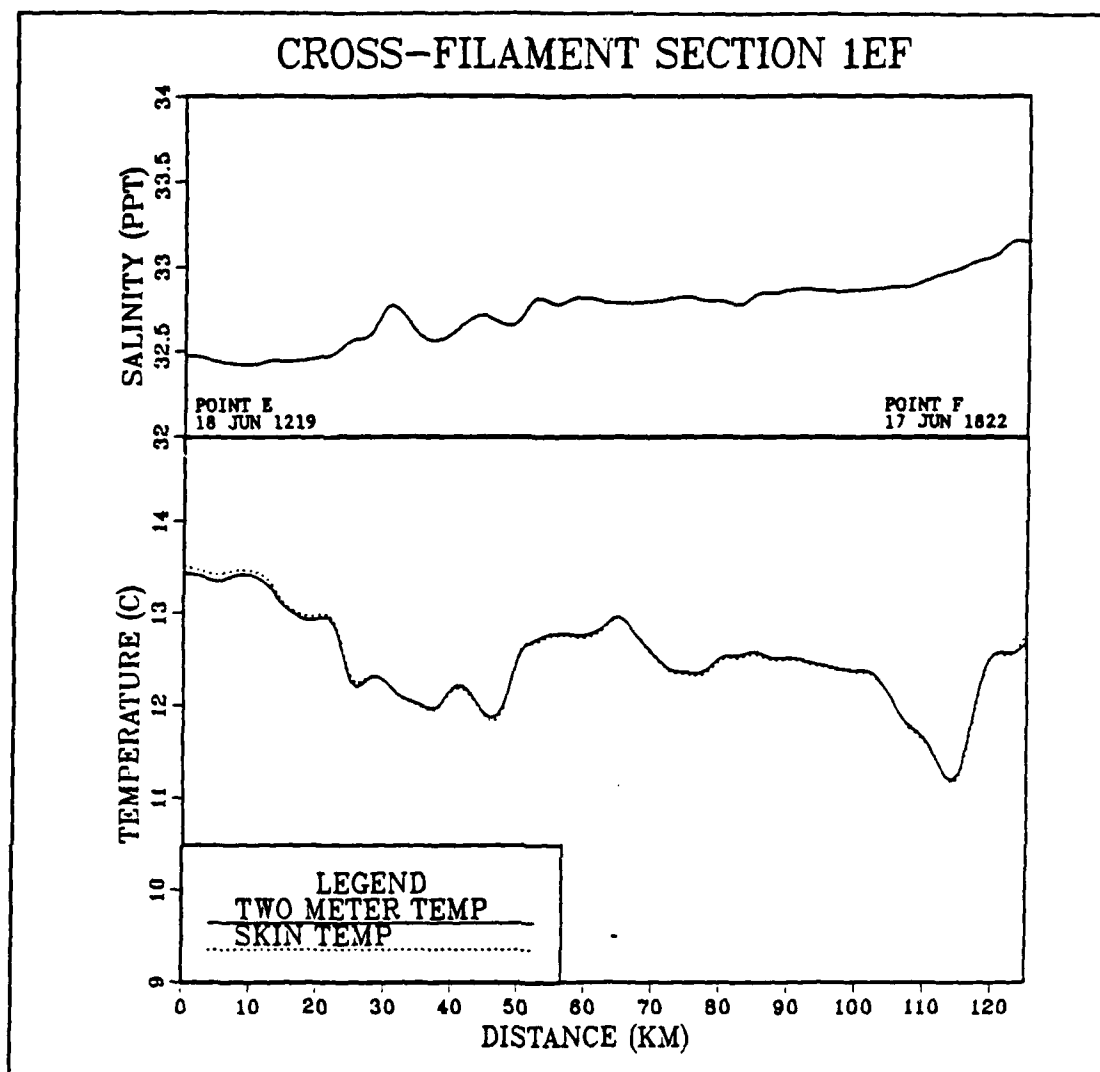


Figure 12. Temperature and Salinity Along Transect 1EF

Between 25 and 55 kilometers, there was a weak signature of a second cold core (filament B). This position corresponds to the cold band (Figure 3) which appears in the imagery to be of northern origin. The minimum temperature was warmer at approximately 12°C. At 12.5°C, the width of the filament was about 30 kilometers. There was a salinity peak near the northern boundary of this filament, but it was less than 10 kilometers wide and it was not readily apparent why it should be isolated in a single peak and not correlated with a temperature signature.

In general, the transect showed two cold filaments with 12.5°C water between them, 12.5 degree water to the south and 13.5°C water to the north. The salinity along the transect showed a gradual increase from 32.5‰ at point E to just over 33‰ at point F. These temperature and salinity characteristics indicate that the southern boundary of filament A was not reached on this leg (Figure 3).

5. Leg 1DC (Figure 13)

This transect began at 1514 on 18 June and ended at 0457 the next day. Between 0 and 25 kilometers, there was evidence of surface heating, corresponding to the hours of daylight during the transect.

At the 25 kilometer point the sea surface temperature dropped from approximately 13.5°C to 12.7°C, marking the northern boundary of a cold filament remnant that was continuous for nearly 100 kilometers to the south. The warm gap visible between filaments A and B (Figure 3) has disappeared and the two filaments are no longer discernable from the surface temperature signal. This is seen more clearly in a later satellite image (Figure 14) taken shortly after the end of the first phase. The strongest temperature gradient at this northern boundary was 0.52°Ckm⁻¹. At the southern boundary, the surface temperature rose from 12.8°C to 14.5°C in a very short distance, with a 0.77°Ckm⁻¹ gradient at the 125 kilometer point. This was the first transect that clearly reached oceanic water to the south, also indicated by the drop in salinity.

Within the boundaries of the cold core, there was also a core of higher salinity extending from 60 to 115 kilometers. While the core of maximum salinity lay within the cold core, only the southern boundary of the filament was common to both. It appears that filaments A and B have the same temperature characteristics, but filament A has a significantly higher salinity. This allows the two to be distinguished from each other and shows that filament B is approximately 30 kilometers in width while filament A is approximately 105 kilometers wide along this transect.

6. Leg 1AB (Figure 15)

The features in this leg were similar to those of the previous leg. A very broad (approximately 70 kilometers) cold filament was present with warmer oceanic water to the north and south. Minimum temperature of the cold filament was now up to about 13°C (from 12.75°C). The salinity did not show the maxima noted previously but did gradually increase from north to south as noted in previous legs, indicating that filament B had not propagated this far offshore. The observations along this leg began at 1136 on 19 June and concluded at 2300. Once again, the effects of daytime heating were

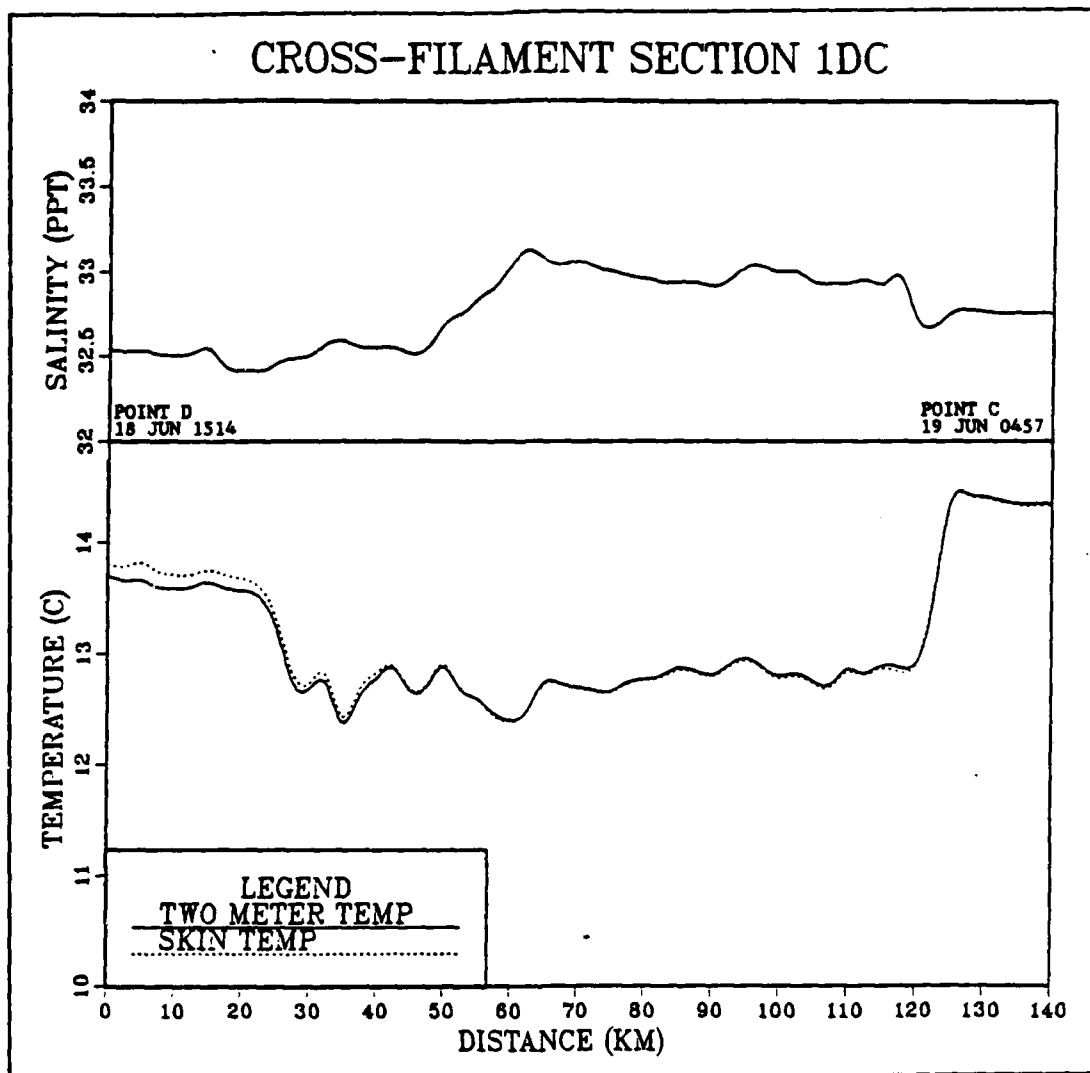


Figure 13. Temperature and Salinity Along Transect 1DC

observed between 50 and 100 kilometers as a small (0.1°C) divergence of the two meter and skin temperatures. The thermal gradient at the north wall (not very well defined) was much weaker at $0.24^{\circ}\text{Ckm}^{-1}$, but the south wall still maintained a strong gradient of $0.52^{\circ}\text{Ckm}^{-1}$.

7. Phase One Summary

Deterioration of any filament with time was anticipated due to mixing processes. Figure 14 shows the phase one track superimposed on 21 June 1987 satellite imagery which was obtained approximately one and one half days after the conclusion of the first



Figure 14. Phase One Track Superimposed on 21 June 1987 AVHRR Imagery

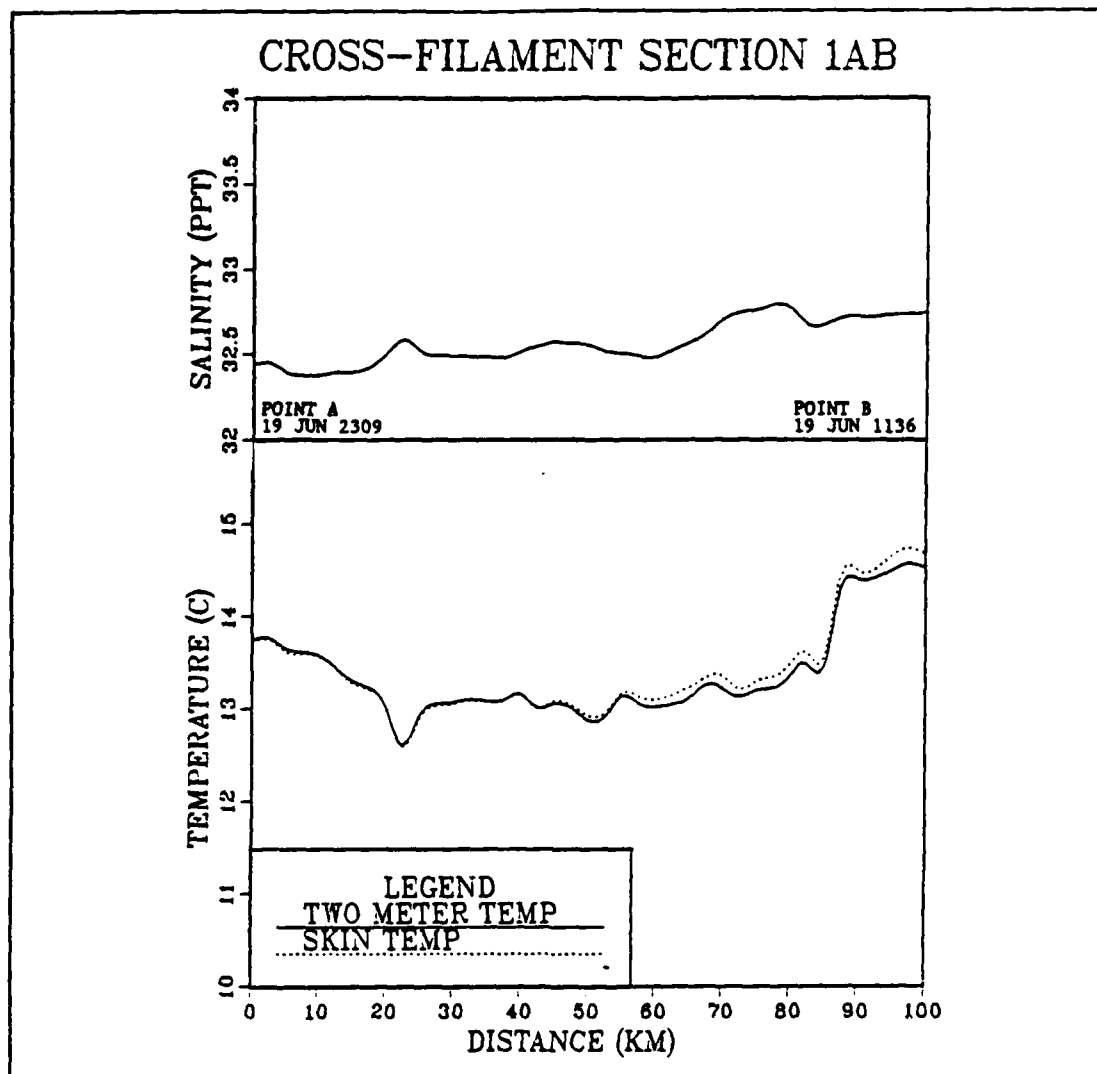


Figure 15. Temperature and Salinity Along Transect 1AB

phase. A comparison of this figure and Figure 3 shows that filaments A and B had merged into a single feature.

The distinguishing characteristics of the three filaments could be described as follows:

- Filament A was the wide region of 12.5°C / 33‰ water which was apparently the remnant of the original filament noted in the pre-cruise imagery and was seen in all the transects except leg 1KL which went through the source waters. Near this older filament were two other filaments which appeared to be younger since they were both colder and more saline than filament A.

- The first of these, filament B was slightly colder than filament A and appeared to have migrated south as an extension of a meander of the coastal upwelling jet originating near Cape Mendocino. It was only seen clearly in leg 1EF and had a characteristic signature of 12°C / 32.7‰. By leg 1DC, it had merged with filament A, and the salinity signature was the only distinguishing characteristic.
- Filament C was the third and coldest of the filaments. It was readily identified in legs 1HG and 1EF and had the sharpest, coldest, most saline signature at 11°C / 33.2‰. This filament was possibly seen first in the satellite imagery of 16 June (Figure 3) as a slight extension of colder water from the source region surrounded by points H, I, L and G. The 21 June image (Figure 14) illustrated that the filament was progressing offshore and was becoming more distinguishable as filament A dispersed. Also shown in this later image was that the leg 1EF cut through filament C was very close to the most seaward tip of the feature which provided an explanation of the weakened (but still sharp) characteristic signature between legs 1HG and 1EF.
- At the seaward limits of filament A, oceanic water was present with a characteristic signature of temperature 13°C or higher and salinity less than 32.5‰.

B. PHASE TWO

After a transit from the most seaward reaches of phase one back to the source waters off Point Arena, the next endeavor and primary goal of the second phase was to relocate the strongest (newest) filament previously identified (filament C) and perform a more detailed survey of it. Figure 4 shows the phase two track and also indicates that the feature of interest extended farther offshore. Figures 16 through 22 are, once again, plots of the continuously monitored variables skin temperature, two meter temperature and salinity along each of the phase two transects.

1. Leg 2IJ (Figure 16)

The R/V POINT SUR arrived at point J at 1450 on 20 June 1987 and commenced a northerly transect through the source region very near the coast. Leg 2IJ (Figure 16) turned out to be one of the most unusual of the entire survey, due to the tremendous temperature difference observed between the skin and two meter sensors. A detailed investigation of this phenomenon is presented in a later chapter. For now, the skin temperature is assumed to be anomalously warm, and only the two meter temperature provided a true indication of any cold filament structure.

The temperatures found in the source region were cold and salinities were high which were similar to results previously noted along leg 1KL. One difference however, was a much greater horizontal variability in the temperature. The coldest water occurred at the 40 kilometer point and was about 10°C. It was confined to a narrow (5-10 kilometer) core and was also concurrent with the maximum salinity of about 33.6‰. At point

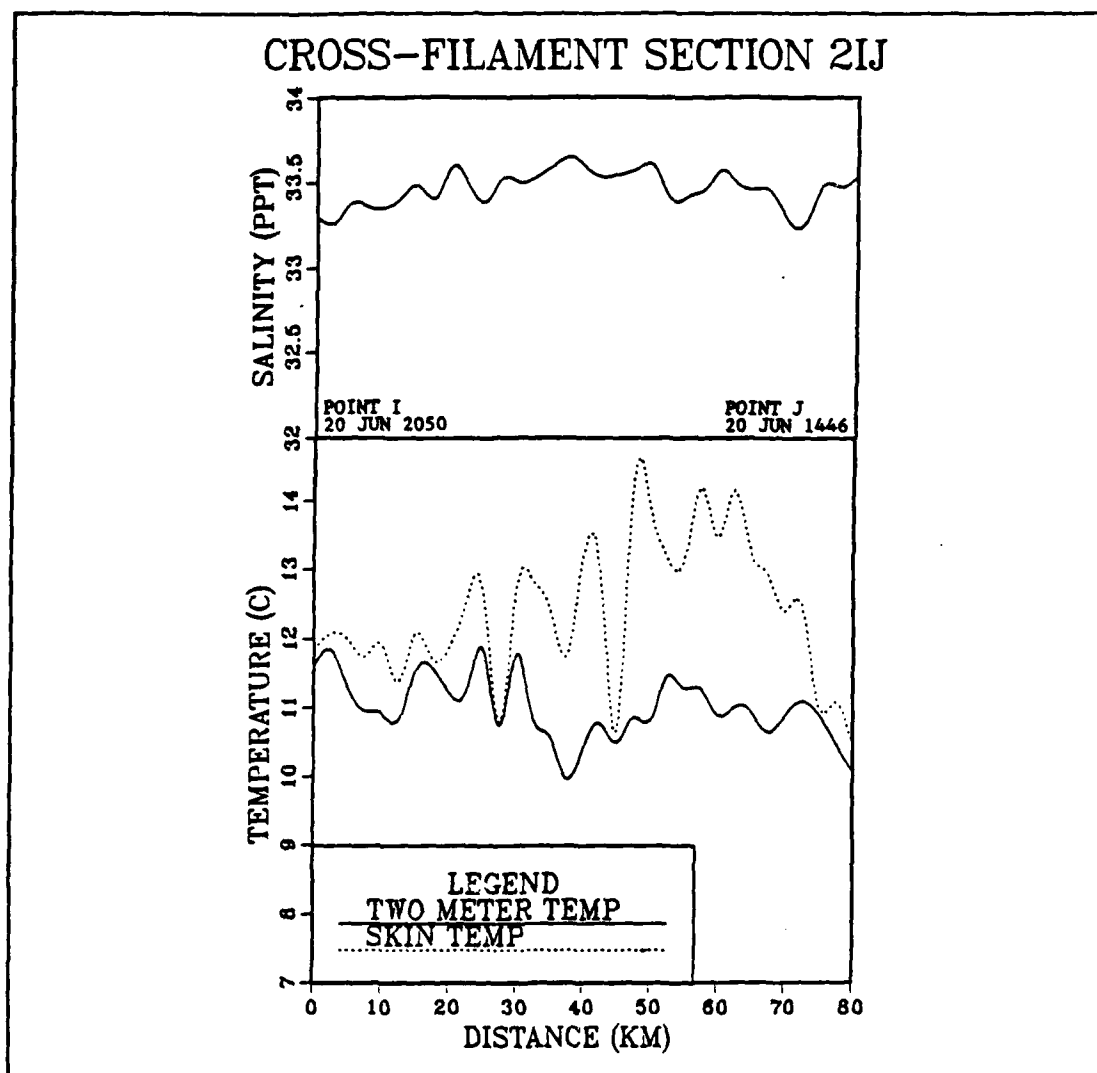


Figure 16. Temperature and Salinity Along Transect 2IJ

J, there was also evidence of an even colder core. This feature though was to the south of filament C and was not investigated.

2. Leg 2HG (Figure 17)

Arrival time at point H was about 2300 on 20 June. Near point H, Figure 4 shows a small filament of relatively cold water extending offshore. This was apparent in Figure 17 between 0 and 10 kilometers but was not a very strong signature for a filament in either temperature or salinity. From 10 to 30 kilometers, there was an intrusion

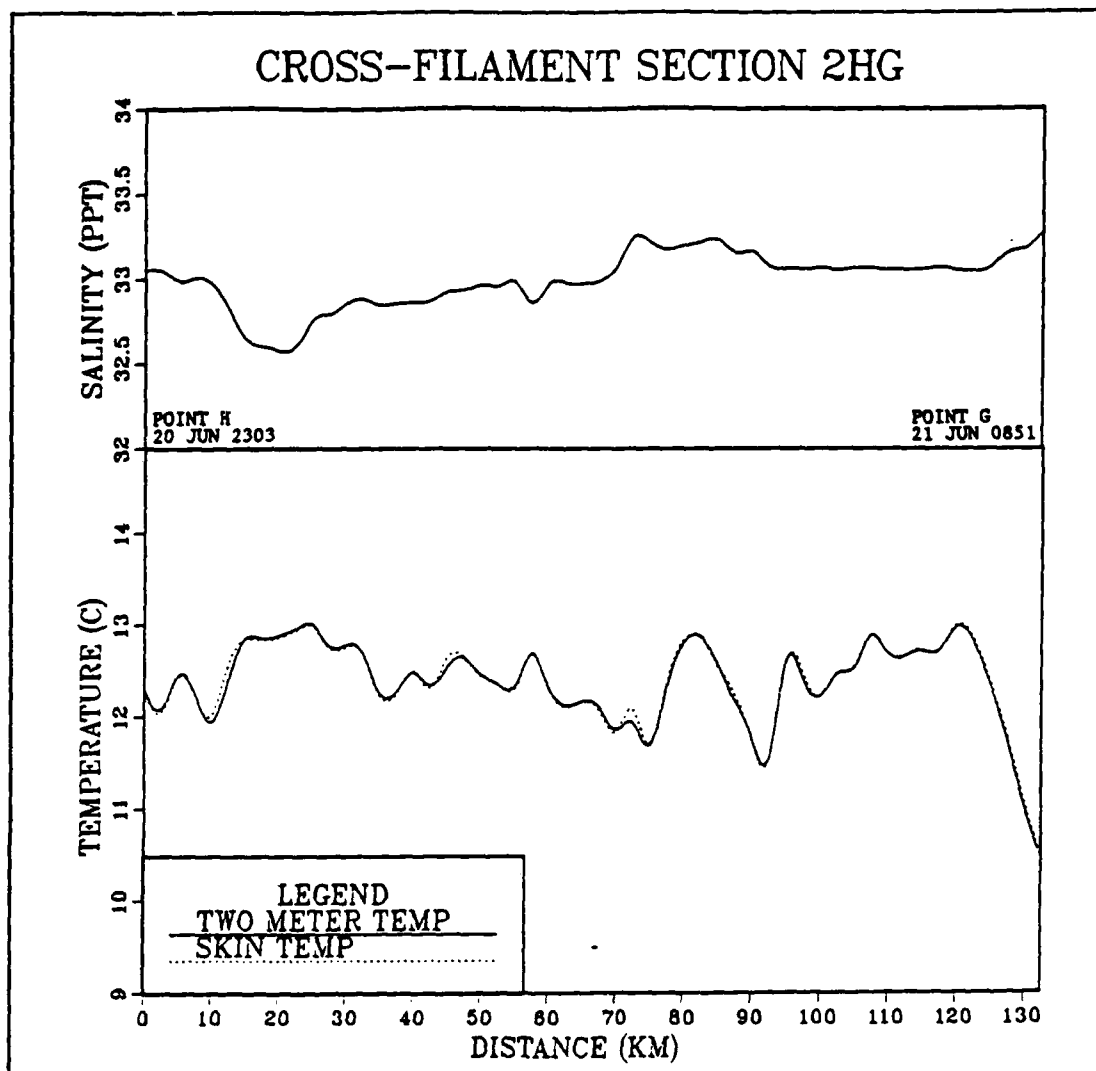


Figure 17. Temperature and Salinity Along Transect 2HG

of relatively warm (13°C) water with a corresponding lower salinity (32.6‰). Continuing southward, there was a steady decrease in temperature and an increase in salinity until about the 75 kilometer point. Based on the imagery in Figure 4, this should be filament C, which appeared to be about 25 kilometers wide along this transect. The signature present was a minimum temperature of 11.5°C and a maximum salinity of 33.6‰. There was an intrusion of warm 13°C water in the middle of the filament (about the 80 kilometer point) which was not visible on the satellite imagery and also showed no corresponding salinity signature. To the south of filament C was a 30 kilometer wide region

of approximately 13°C and 33.1‰ water. Near point G, there was a rapid rise in salinity coupled with an even more rapid drop in temperature associated with a region of very cold surface temperatures clearly visible on Figure 4 near points F and G. This appeared to be the beginning of another filament originating to the south of filament A near Point Reyes, which was not investigated.

3. Leg 2EF (Figure 18)

Leg 2EF began at 1143 and ended at 1914 on 21 June, and the satellite image in Figure 4 was taken at 1351 the same day. Point F was just at the edge of the very cold feature that was seen near point G but there was only a small indication of cooler temperature and no unique salinity signature. Filament C can easily be distinguished on the temperature plot between 10 and 30 kilometers. The minimum temperature was 11.3°C, but there was only a very slight salinity maxima of 33.3‰ between 20 and 30 kilometers (only the southern portion of the filament). The filament width was approximately 20 kilometers with a north wall gradient of 0.28°Ckm⁻¹ and a south wall gradient of 0.68°Ckm⁻¹. The surface water to the south was mostly 12.5°C and 33.1‰. To the north, the water was slightly warmer and less saline at 12.8°C and 32.8‰. Diurnal heating at the surface was apparent along most of the transect.

4. Leg 2ED (Figure 19)

Once again, filament C was a very prominent feature on the temperature plot between the 20 and 40 kilometer points. The minimum temperature was along the southern boundary of the filament at 11.1°C. The salinity signature was broader and was located between the 20 and 45 kilometer points. The salinity maximum was also along the southern boundary of the filament at 33.2‰. The northern boundary was characterized by a more gradual rise in temperature (0.48°Ckm⁻¹) and a more gradual drop in salinity (0.06‰km⁻¹) than at the southern boundary (0.80°Ckm⁻¹ and 0.10‰km⁻¹). The filament was bordered to the north and south by roughly 12.6°C and 32.8‰ water. There were also significant atmospheric events occurring along this leg. After crossing the filament (just past the halfway point) the wind and sea conditions were deemed too rough to attempt any additional CTD casts as part of the mapping effort on filament C. Filament mapping did continue however, using the continuous surface monitoring instruments and the ADCP.

5. Leg 2CD (Figure 20)

Filament C remained the most prominent feature across this transect. However, the signature had weakened significantly. The minimum temperature increased to

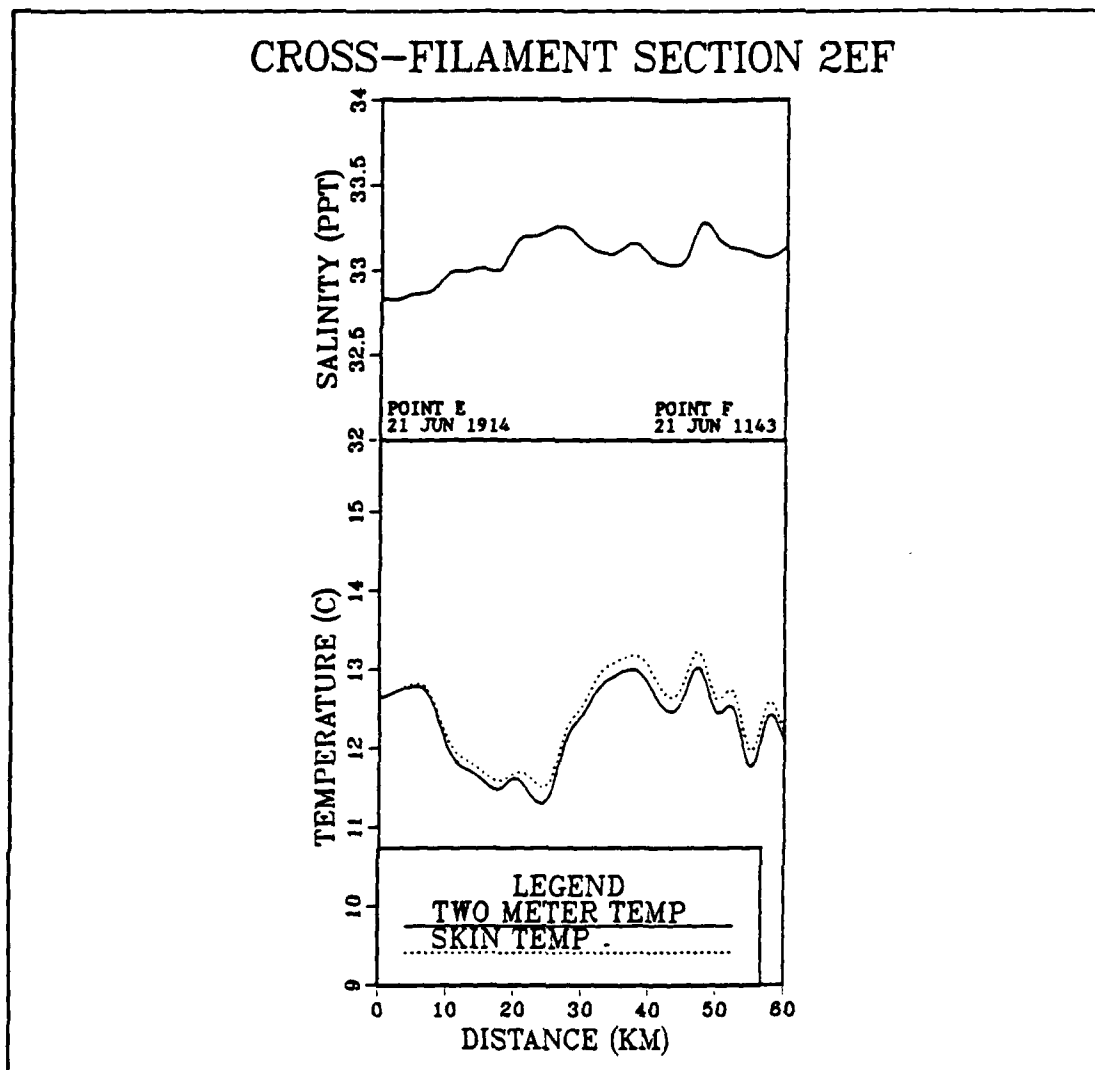


Figure 18. Temperature and Salinity Along Transect 2EF

11.5°C, while the maximum salinity decreased slightly to about 33.1‰. There was no apparent offset between the temperature or salinity maxima, and the north and south boundaries appeared to be symmetrical. Temperature gradients across both filament boundaries weakened with the north wall at $0.23^{\circ}\text{Ckm}^{-1}$ and the south wall at $0.34^{\circ}\text{Ckm}^{-1}$. Salinity gradients were similar to the previous leg with the north wall at 0.04‰km^{-1} and the south wall much stronger at 0.17‰km^{-1} . Filament width was dependent upon which isotherm was chosen as being representative. At the 12.0°C isotherm, the width is approximately 12 kilometers. The surface water to the north was

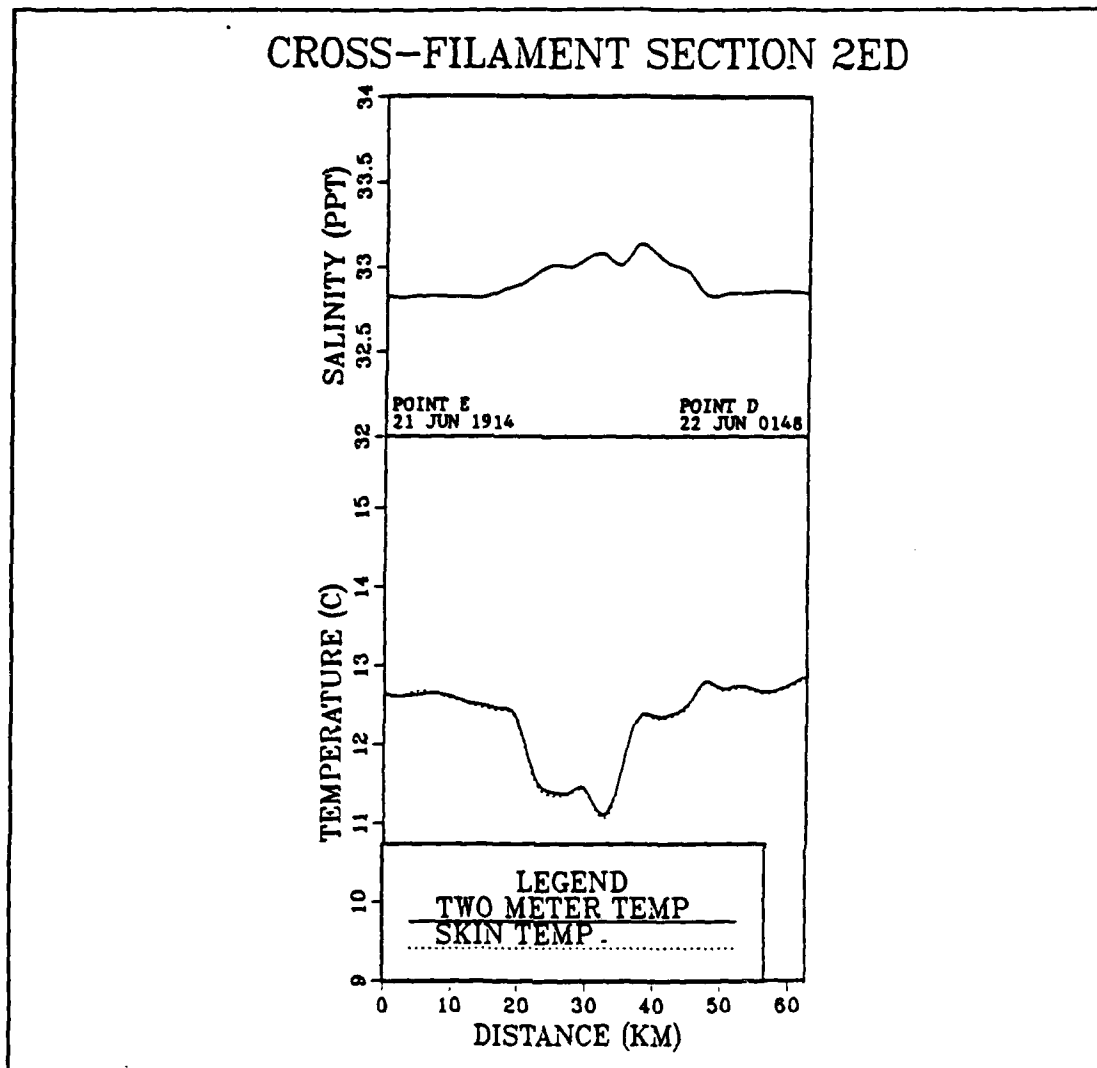


Figure 19. Temperature and Salinity Along Transect 2ED

still at about 12.5°C and 32.8‰. The water to the south had the same salinity, but it had warmed to about 13°C.

6. Leg 2CB (Figure 21)

The prominent feature along this transect that marked the position of filament C was the narrow salinity peak at about the 40 kilometer point. The maximum of 33.1‰ was very obvious because it was bounded to the north and south by less saline 32.8‰ water. There was a minimum signal of about 12°C near 40 kilometers but not nearly as sharp a signal as any of the previous legs. Even with the increased winds and seas, there was

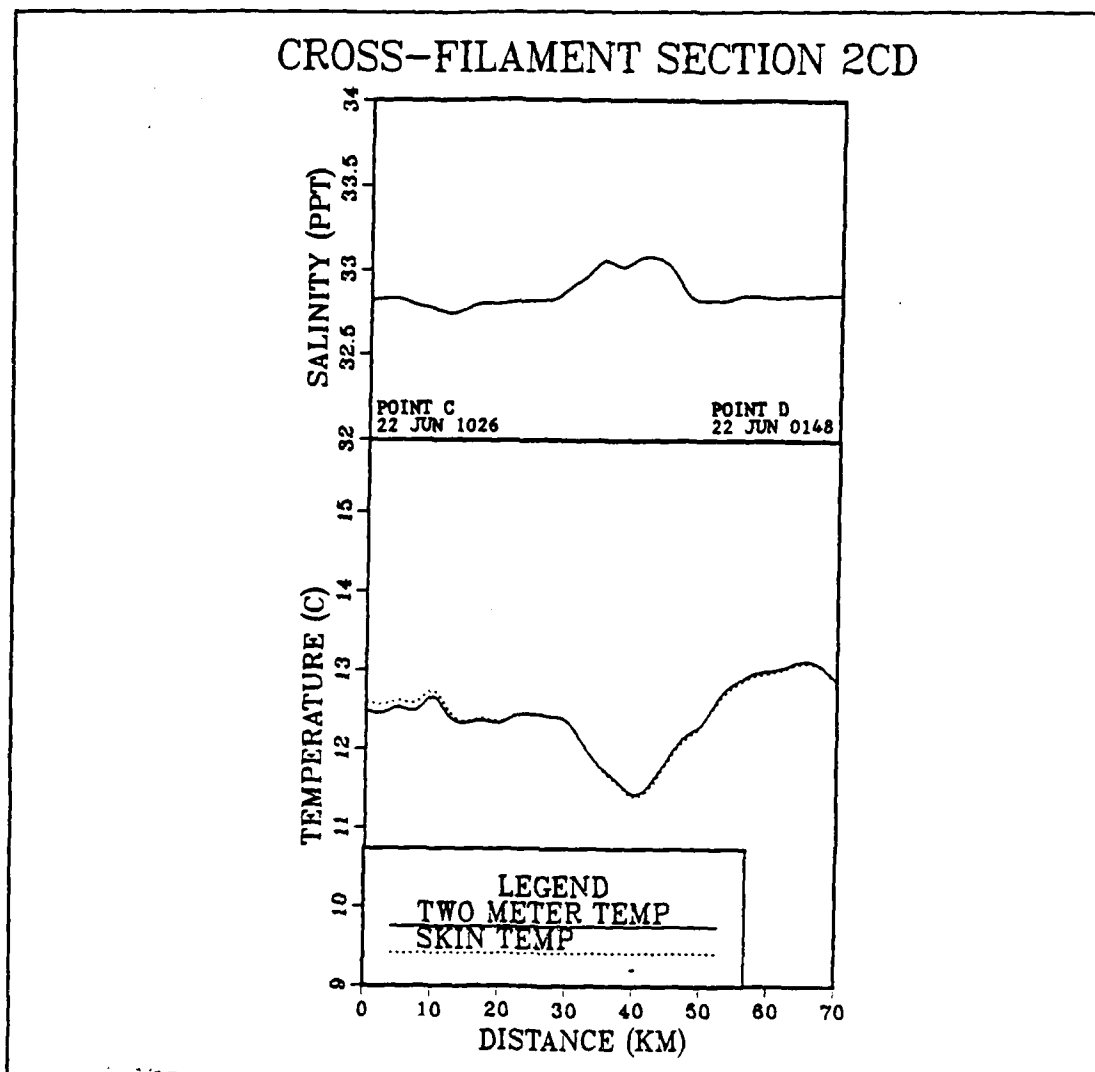


Figure 20. Temperature and Salinity Along Transect 2CD

still a noticeable daytime heating difference between the skin and two meter temperatures, which likely contributes to the diurnal disappearance of the surface temperature minimum as the filament moves offshore.

7. Leg 2AB (Figure 22)

The salinity signature was once again the strongest indication of filament C along this transect. Between 10 and 20 kilometers the familiar 33.1‰ signature was present. A very weak temperature signal was seen at 10 kilometers (12°C). The surface water immediately bordering the filament was becoming more characteristic of oceanic

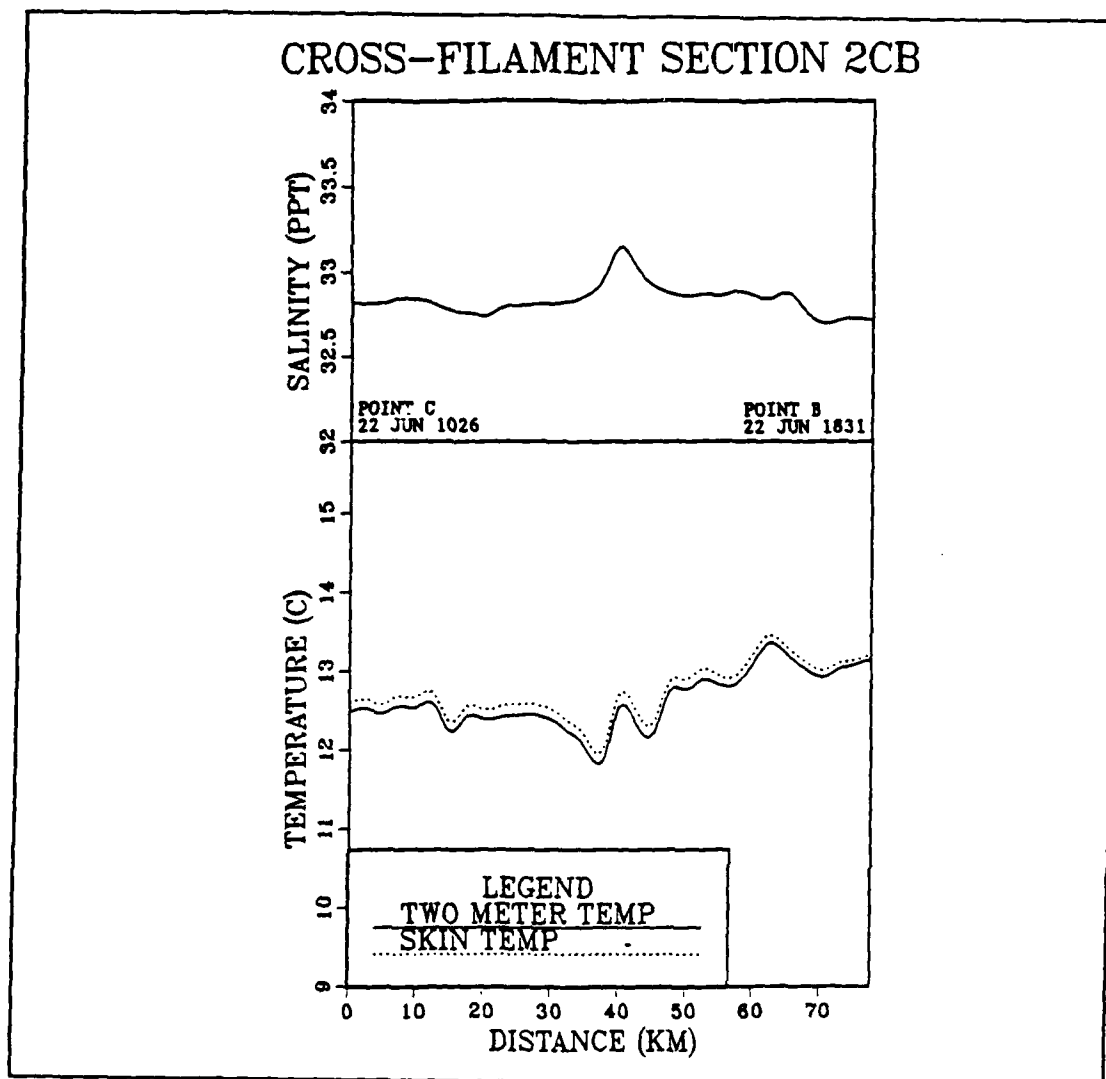


Figure 21. Temperature and Salinity Along Transect 2CB

water as its temperature increased and salinity decreased. There was no longer a significant minimum in the surface temperature.

Point A was reached at 0728 on 23 June with weather conditions worsening still. Winds exceeding 40 knots with gusts to 50 knots and a forecast of even worse weather to come forced the R/V POINT SUR to steam to shelter at Drake's Bay. The ship arrived there at 1803 on 23 June and remained until 2357 on 24 June when weather reports indicated workable conditions offshore.

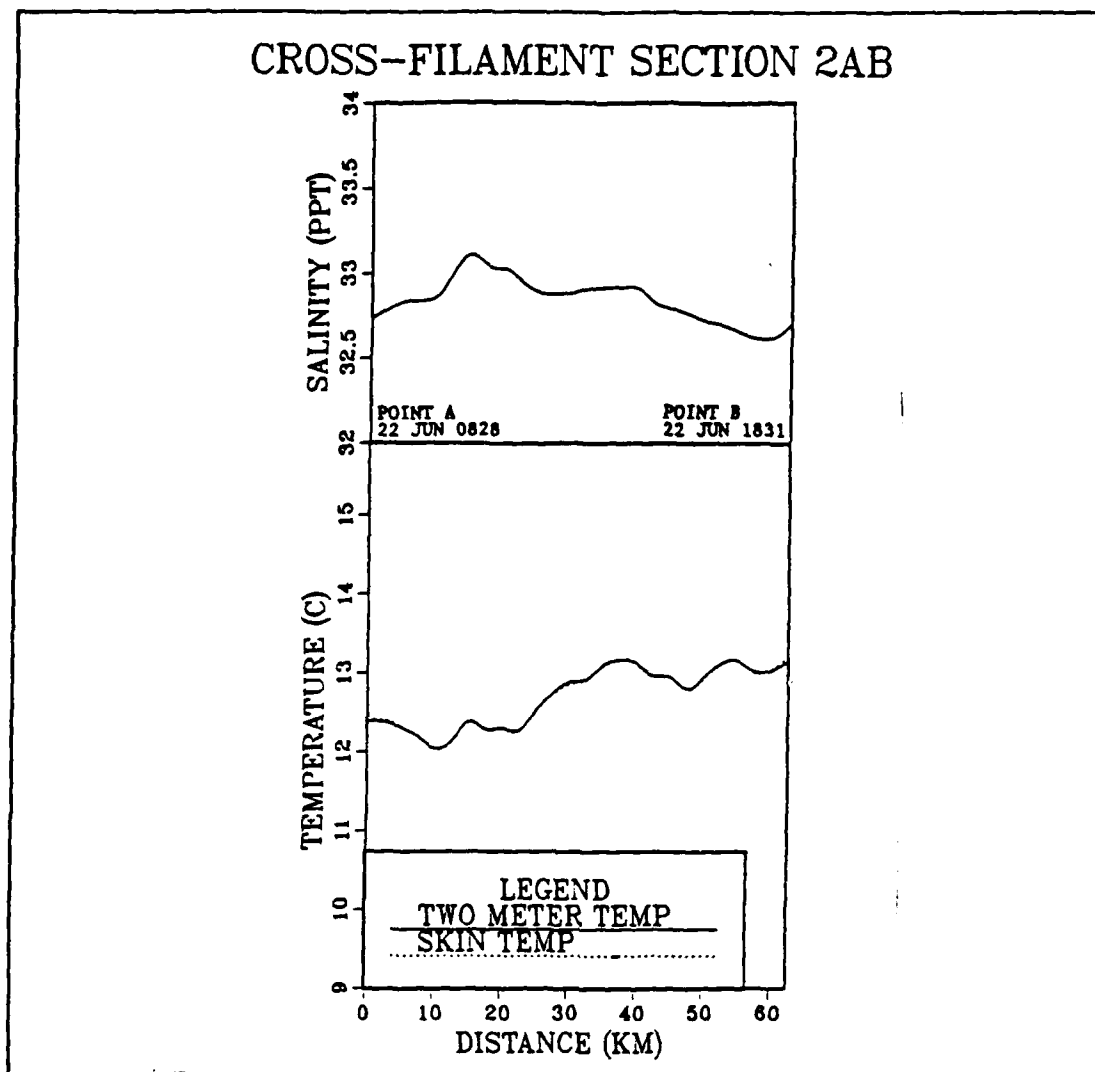


Figure 22. Temperature and Salinity Along Transect 2AB

8. Phase Two Summary

During the second phase, filament C was successfully relocated and mapped. The evolution of the surface features of filament C was evident in the satellite imagery previously introduced as Figures 3 and 4. In Figure 3, the filament had just started to separate from the coastal upwelling region just south of Point Arena. Figure 4 shows progression offshore while maintaining a narrow, filamentous shape.

Over the four and one half days between satellite images, the filament progressed approximately 55 kilometers offshore. As a first approximation, the offshore

propagation speed was $\sim 14.0 \text{ cm s}^{-1}$ as determined from the imagery. Geostrophic velocities relative to 500 decibars, calculated by P. Jessen at NPS using CTD data which correlated to filament C, were 7.5 cm s^{-1} for leg 1HG, 15.0 cm s^{-1} for leg 1EF and 35.0 cm s^{-1} for leg 2EF. The transects are very nearly perpendicular to the strike of the offshore movement of the filaments, so the calculated geostrophic velocities should be accurate. If anything, they will be a slight underestimate if the transect is not quite perpendicular to the flow due to unresolved vector components. The position of the geostrophic jet corresponds to the position of filament C, but the 10 kilometer spacing of the CTD stations makes it impossible to define the location of the maximum currents within the filaments. Once the ADCP data is processed and can be fully correlated with both the horizontal and vertical sections, the exact locations and strengths of currents within the filaments can be determined. Geostrophic velocities were not available for the remainder of the phase two legs due to cessation of CTD stations as the weather worsened. Flament *et al.* [1985] made similar estimates of filament surface velocities from satellite imagery during CODE. They arrived at values of $\sim 50 \text{ cm/s}$ but *in situ* measurements of the same feature indicated surface velocities of $\sim 80 \text{ cm/s}$ [Davis, 1985; Kosro and Huyer, 1985].

Table 2 presents significant measurements of identifying variables of filament C for both phase one and phase two. The data is for those transects where the filament was clearly identifiable. The filament was traceable by a fairly constant signature with a temperature minimum between 10.8 and 11.5°C and a salinity maximum between 33.1 and 33.3‰ . Temperatures tended to rise with increasing distance offshore and salinity showed a very slight decrease. Distance offshore also coincides with an increase in time so the temperature increase and salinity decrease are most probably due to surface heating and mixing processes. Huyer and Kosro [1987] show that an offshore temperature increase and salinity decrease are consistent with nearshore upwelling processes but Huyer [1983] also cautions that observations may vary depending on the rate of heating and mixing as well as the rate of upwelling. The filament width was almost constant at 15-25 kilometers which is consistent with the findings of Huyer [1983], who equated cold filament width with the Rossby radius of deformation for latitudes off Northern California. Other studies of cold filaments such as Flament *et al.* [1985], Kosro and Huyer [1986] and Brink [1987], also agree with a basic width measurement of cold filaments off Point Arena of 10-30 kilometers. The temperature gradient across the southern boundary was consistently much stronger than across the northern filament

Table 2. SIGNIFICANT MEASUREMENTS OF FILAMENT C: Made during phase one and phase two during all the transects in which filament C was clearly distinguishable.

TRANSECT	$T_{\text{min}}(^{\circ}\text{C})$	S_{max} (PPT)	WIDTH (KM)	SOUTH WALL GRADIENT ($^{\circ}\text{C}/\text{KM}$)	NORTH WALL GRADIENT ($^{\circ}\text{C}/\text{KM}$)
IHG	10.8	33.1	25	0.98	0.30
IEF	11.3	33.1	15	1.15	0.25
2EF	11.3	33.3	20	0.68	0.28
2ED	11.1	33.2	20	0.80	0.48
2CD	11.5	33.1	20	0.34	0.23

boundary. The strongest gradients for both boundaries were observed at a point approximately 35 kilometers offshore and from there, both gradients showed a steady weakening with increased distance offshore. The observed offshore maximum could be caused by a disruption of the source waters due to a wind relaxation event, but further study and comparisons of all the pilot survey data are required to gain further insight into possible causes. These results are consistent with other filament studies [Flament *et al.*, 1985; Brink, 1987], but with the finer resolution available using the continuous monitoring surface sensors, a very accurate quantitative measure of the surface gradients was obtained.

C. PHASE THREE

The third and final phase of the survey began after the adverse weather conditions from the second had subsided. Recovery of the specially instrumented surface drifter package was the only absolute requirement. Beyond that, roughly two and one half days were available for continued filament mapping. Unfortunately, the storm system that forced the abrupt end of phase two also brought with it extensive cloudiness which dominated the entire region from 23 June through the end of the survey period. There were also no periods of cloud-free conditions until well after the survey had concluded so subsequent satellite imagery was not useable to verify or infer possible filament location. Therefore, with the total lack of satellite imagery for guidance together with the unknown effect of the intense storm on the surface features, it was decided to use the

remaining time to revisit some of the legs of phase two where filament C was seen earlier to be very prominent. Hopefully, the information obtained could provide insight into filament propagation and dissipation with time. Figure 5 shows the phase three track superimposed on the last available satellite image from June 1987. It is clear that there was already extensive cloud contamination in the survey area which effectively masked any surface signature of cold filaments. Figures 23 through 26 show the surface temperature and salinity plots along the transects of phase three.

1. Leg 3BA (Figure 23)

After recovery of the surface drifter at 1416 on 25 June (near point A), a northerly transect commenced which would overlap the phase two transect 2CB. The transect was completed at 0456 on 26 June. Between 100 and 115 kilometers, there was a small feature which looks a little like a filament except that there was no salinity maximum to go along with the observed temperature minimum of 12.7°C . Also, the north wall gradient was slightly stronger than that at the south wall with values of $0.28^{\circ}\text{Ckm}^{-1}$ and $0.15^{\circ}\text{Ckm}^{-1}$ respectively. Continuing north, a very sharp temperature drop from 13.5 to 11.6°C was observed near the 45 kilometer point. The gradient at this point was $0.62^{\circ}\text{Ckm}^{-1}$. The very cold surface water persisted for only five kilometers then warmed to slightly over 12.0°C . The surface temperature then varied between 12.0 and 12.5°C over the rest of the transect. The salinity maxima was seen at the 25 kilometer point, measured at 33.0‰ . There was also a slight peak at the 45 kilometer point corresponding to the temperature minimum, but the measured value of 32.8‰ is very low for the observed temperature suggesting that its origin is probably not freshly upwelled water.

2. Leg 3BC (Figure 24)

This transect began at 0456 on 26 June and concluded at 1916 the same day. The features along leg 3BC were almost identical to those observed along the northern half of leg 3BA. To the south, water greater than 13.0°C and salinity less than 33.0‰ was found. At the 45 kilometer point, there was a rapid drop in temperature to 11.4°C with a slight salinity peak but not the salinity maxima. The temperature gradient at 45 kilometers was very strong at $1.66^{\circ}\text{Ckm}^{-1}$. The salinity maximum of 33.0‰ was observed approximately 20 kilometers north of the temperature minima.

3. Leg 3DC (Figure 25)

The transect along leg 3DC covered approximately the same area as leg 2ED. The survey began at 1916 on 26 June and finished at 0158 on 27 June. Unlike the

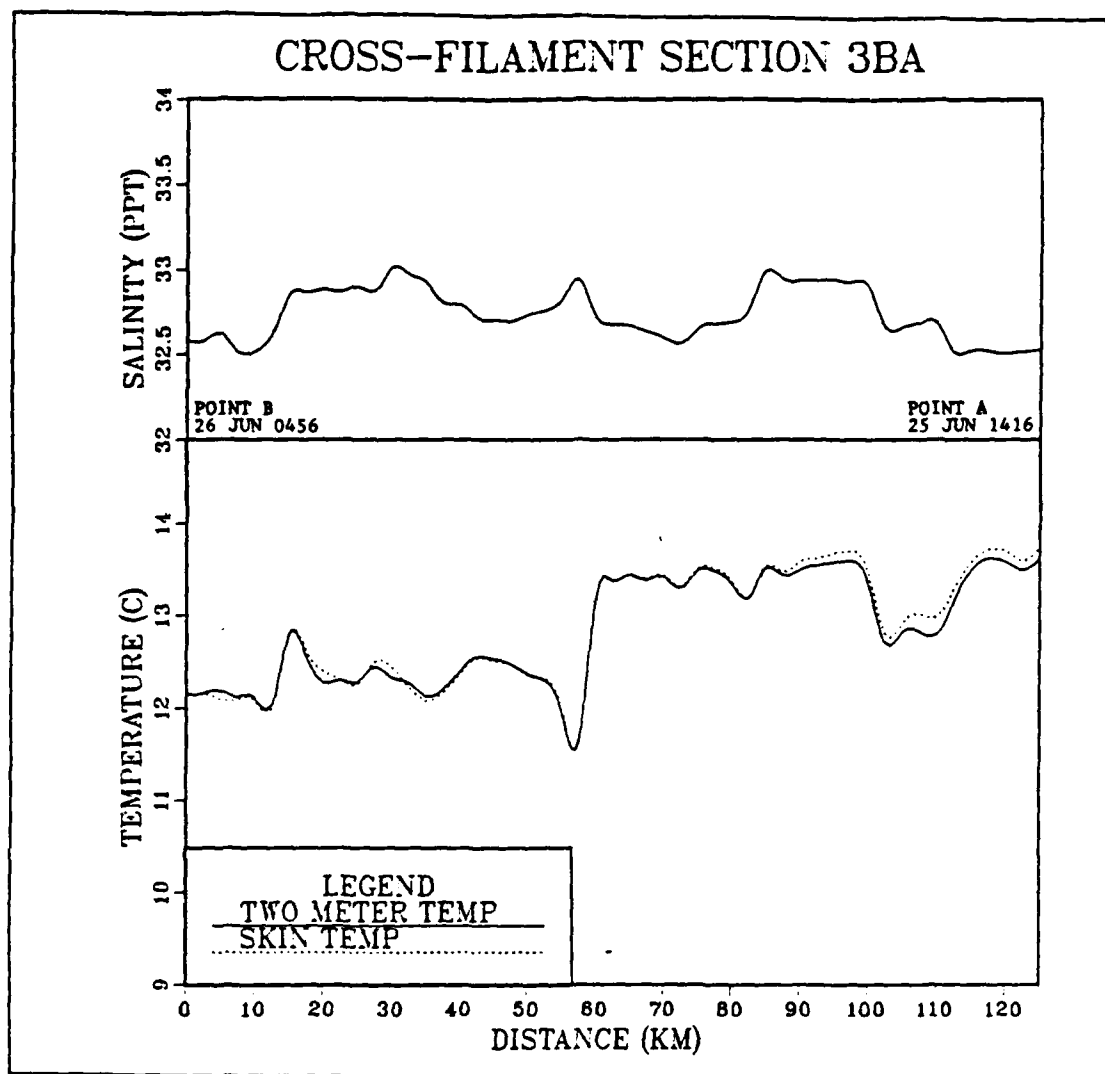


Figure 23. Temperature and Salinity Along Transect 3BA

previous transects, there were no observed features that resembled filament-like structure. There was much variability in the surface temperature field with many observed peaks and valleys and there was correlation with miniscule salinity peaks and valleys, but there was no indication of a filament which might be continuous with the previous two legs. One feature that did stand out was a narrow region of oceanic water between 50 and 65 kilometers. The feature was much warmer (13.8°C) than the surrounding water and the drop in salinity to 32.6‰ was the only region where salinity did not remain fairly constant.

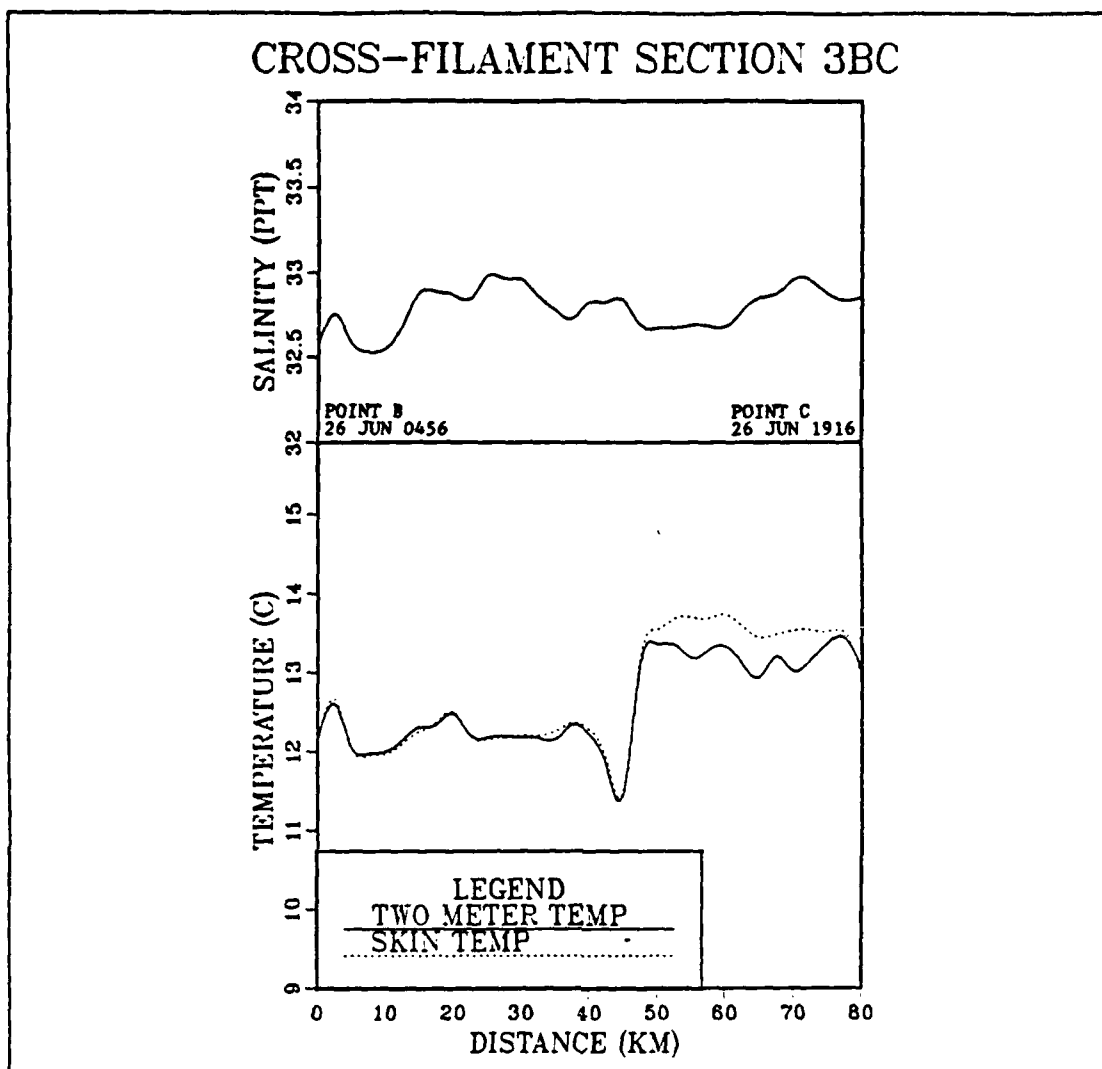


Figure 24. Temperature and Salinity Along Transect 3BC

4. Leg 3EF (Figure 26)

Following a short period during which several more surface drifting buoys were deployed, the final transect of the survey, covering most of the phase two leg 2HG, was made. It began at 2303 on 20 June and was completed at 0851 the next morning. The results were similar to leg 3DC in that there was a very confused picture with no apparent organization or signature of features seen previously. Temperature was variable, mostly between 12.0 and 13.0°C, to the north and greater than 13.0°C to the south. Salinity varied more than in the previous transect. Although most of the time it was

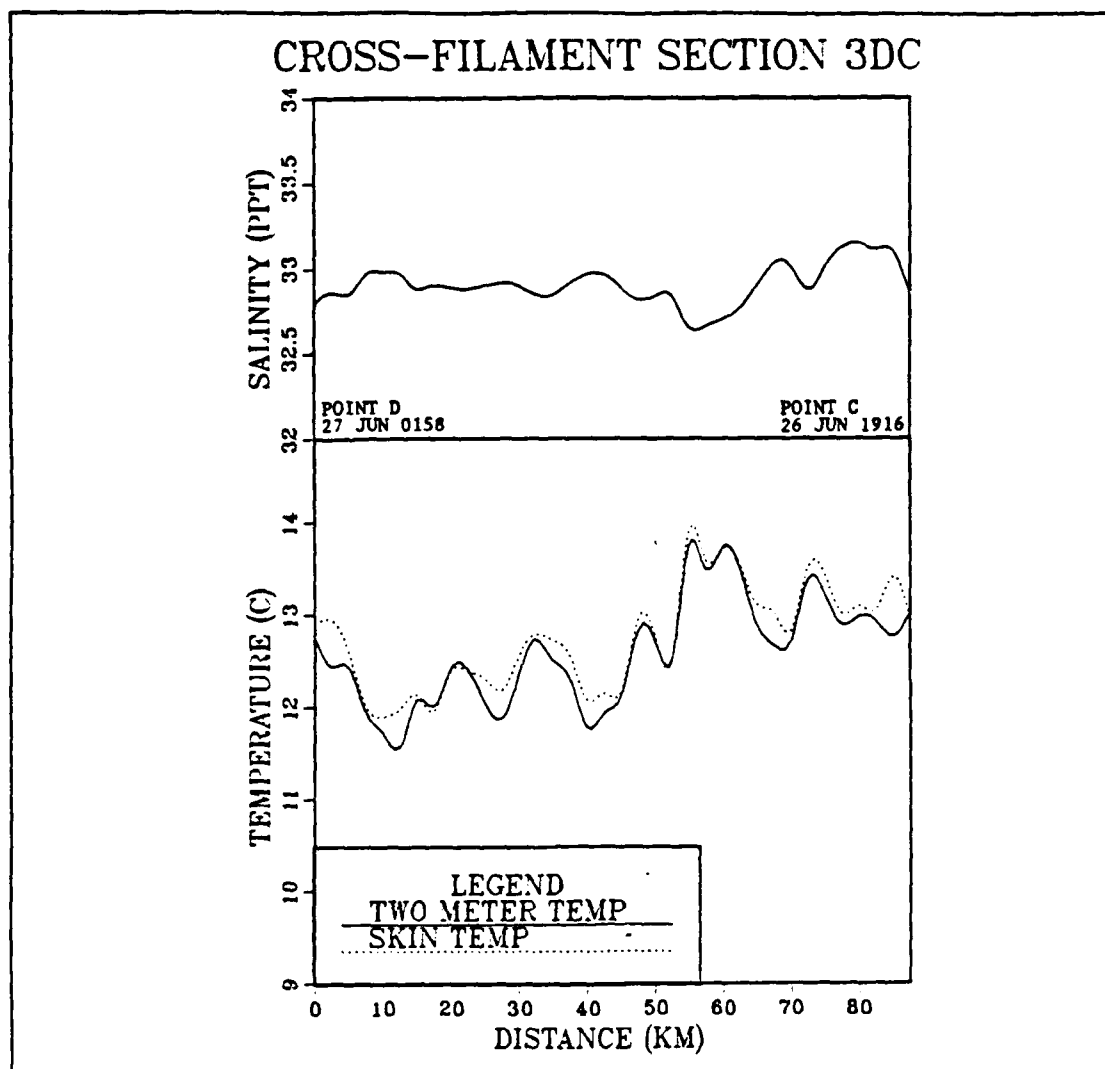


Figure 25. Temperature and Salinity Along Transect 3DC

about 33.0‰, there were three distinct, narrow peaks of higher salinity (33.4 to 33.5‰). Each of these salinity peaks also correlated to three distinct, narrow regions of temperature minima (less than 12.0°C).

5. Phase Three Summary

By the time mapping could be continued in phase three, there was no evidence of filament C. The first observation of filament C was in imagery from 16 June (Figure 3), and the last time it was observed was during the phase two transect along leg 2CD on 21 June. Some time between then and the leg 3BA transect on 25 June, the surface

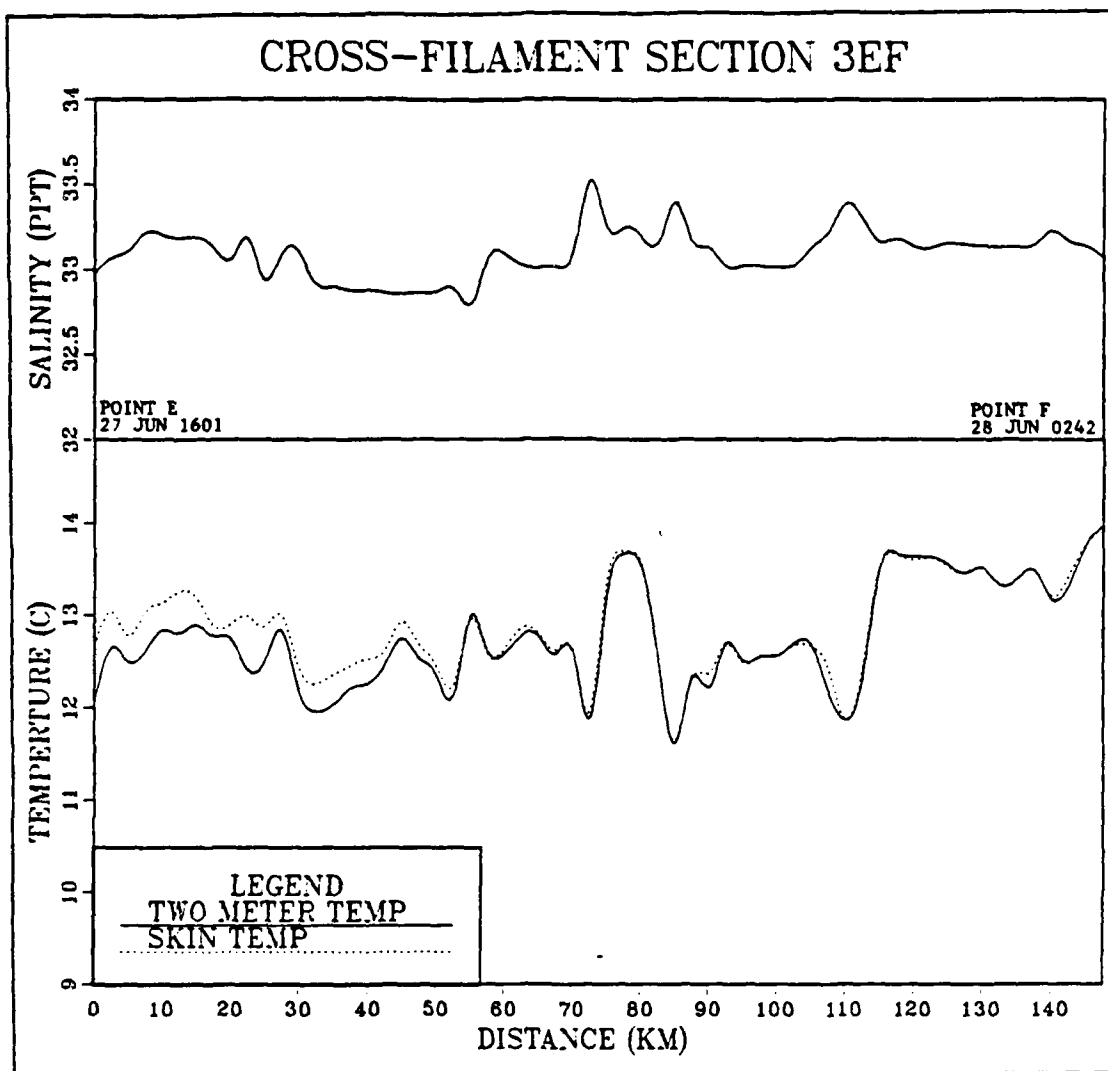


Figure 26. Temperature and Salinity Along Transect 3EF

features of the filament had completely vanished. The apparent lifetime of this particular filament was 5-10 days.

D. SEA SURFACE TEMPERATURE ANOMALY

The second phase of the survey provided observations of very intense surface heating during the initial leg. This transect (between points I and J, Figure 2) began after a transit from the most seaward stations of the first phase back to the near coastal region to once again search the source waters for evidence of new filaments. A generally

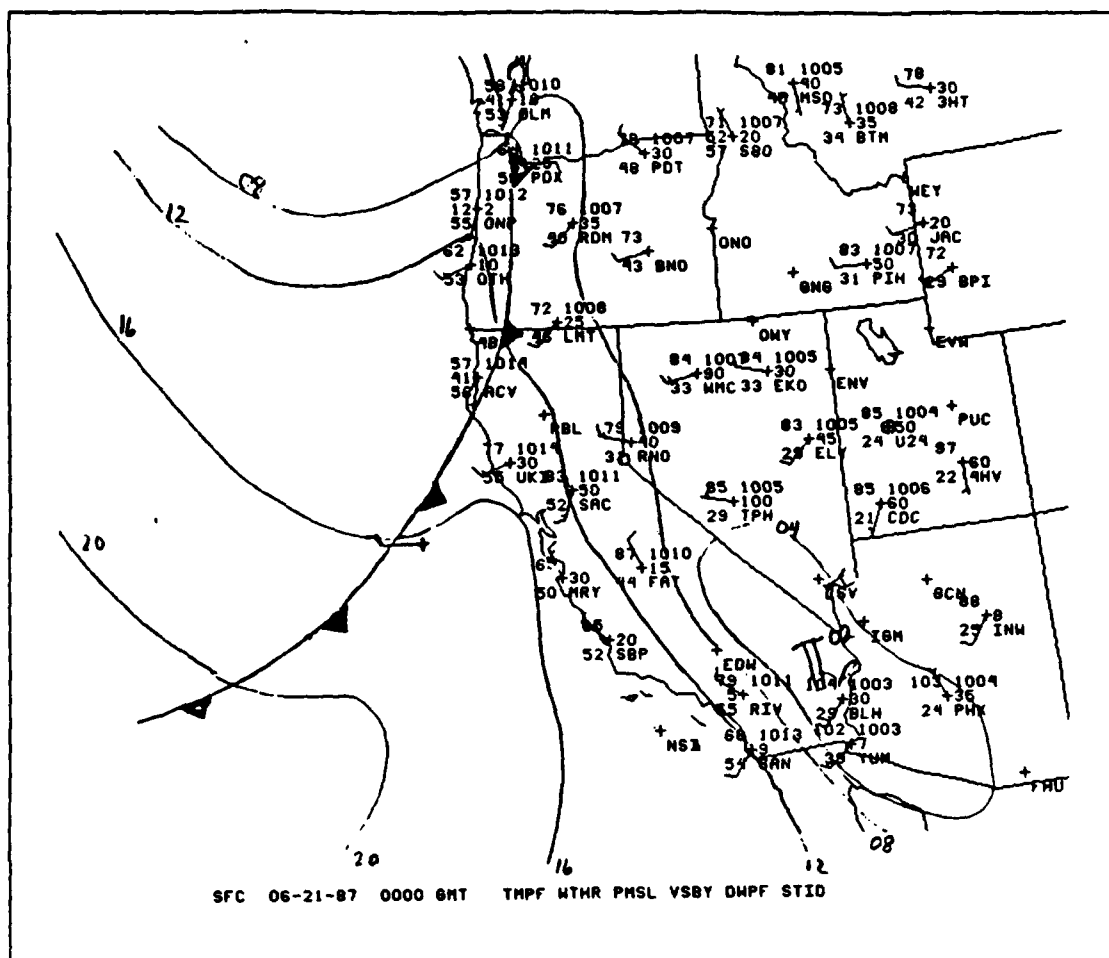
northward alongshore course was maintained to follow the 100 meter isobath and remain roughly perpendicular to the offshore strike of any potential filaments.

Figure 27 shows the 00Z National Meteorological Center (NMC) surface weather analysis for June 21, 1987 (1300 local time on the 20th of June). This analysis indicates that the region was being influenced by a weak cold front associated with a low pressure system in the Gulf of Alaska. The very wide isobar spacing resulted in a weak pressure gradient which reduced wind speeds both in front of and behind the frontal system. Cloudiness associated with the passage of this cold front obscured satellite imagery for sea surface temperature determination and filament location after the 22nd of June.

Local observations from R/V POINT SUR indicated light, variable winds under clear skies in the morning, changing to light southerly winds under broken stratus and stratocumulus clouds associated with the frontal passage. In the absence of appreciable winds, the sea surface was very flat and glassy. Local conditions are shown in a photograph taken during the afternoon from the deck of the POINT SUR (Figure 28). A feature readily apparent is the "patchy" nature of the surface roughness. Alternating expanses of completely calm, glassy regions are interspersed with areas showing evidence of very small ripples or capillary waves.

As the R/V POINT SUR transited through the region of patchiness, the skin temperature readings monitored on the SDAS CRT began to vary significantly from the two meter readings. Figure 16 from the second phase shows a plot of skin and two meter temperatures for the period 1450 to 2050 on the 20th of June while transiting between points I and J. As with most of the transect legs described earlier, this was not a continuous transit due to several short stops to make CTD casts. Since the boom probe had a tendency to sink when the ship was stopped, the data for periods when the ship was on station was deleted. Over this six hour period, the mean difference between the skin and two meter temperatures was 0.92°C with a variance of 1.86°C^2 . This was an extremely high variance when compared to earlier calculations such as those along leg 2AB where the variance was only $0.00084^{\circ}\text{C}^2$. The processes causing the anomalous temperature differences were apparently occurring only in the very near surface layer.

The maximum difference noted between the skin and two meters was 4.7°C and occurred at 1606 local time. There were many other maxima in temperature difference along the track, and these are compiled in Table 3. The most distinctive peaks appear to have spatial scales of about ten kilometers, while there are smaller fluctuations seen to be as little as one kilometer apart (Figure 16). The magnitude of the temperature



difference peaks ($\Delta T = T_{skm} - T_{2m}$) increased monotonically from 1428 to 1606 and decreased thereafter. The peaks are separated by regions where $\Delta T = 0$ (i.e., there were no anomalous surface effects at all). Note that deletion of the data during periods when the ship was stopped indicate that the fluctuations were not due to the boom probe sinking and rising as the ship stopped and started.

It is hypothesized that these large differences between the skin and two meter temperatures can be explained by surface heating due to solar insolation alone, which on a very calm day, is trapped in a surface microlayer that is less than two meters deep. To test this hypothesis, a heat budget for the upper ocean during the period of daytime heating on 20 June 1987 is considered below.

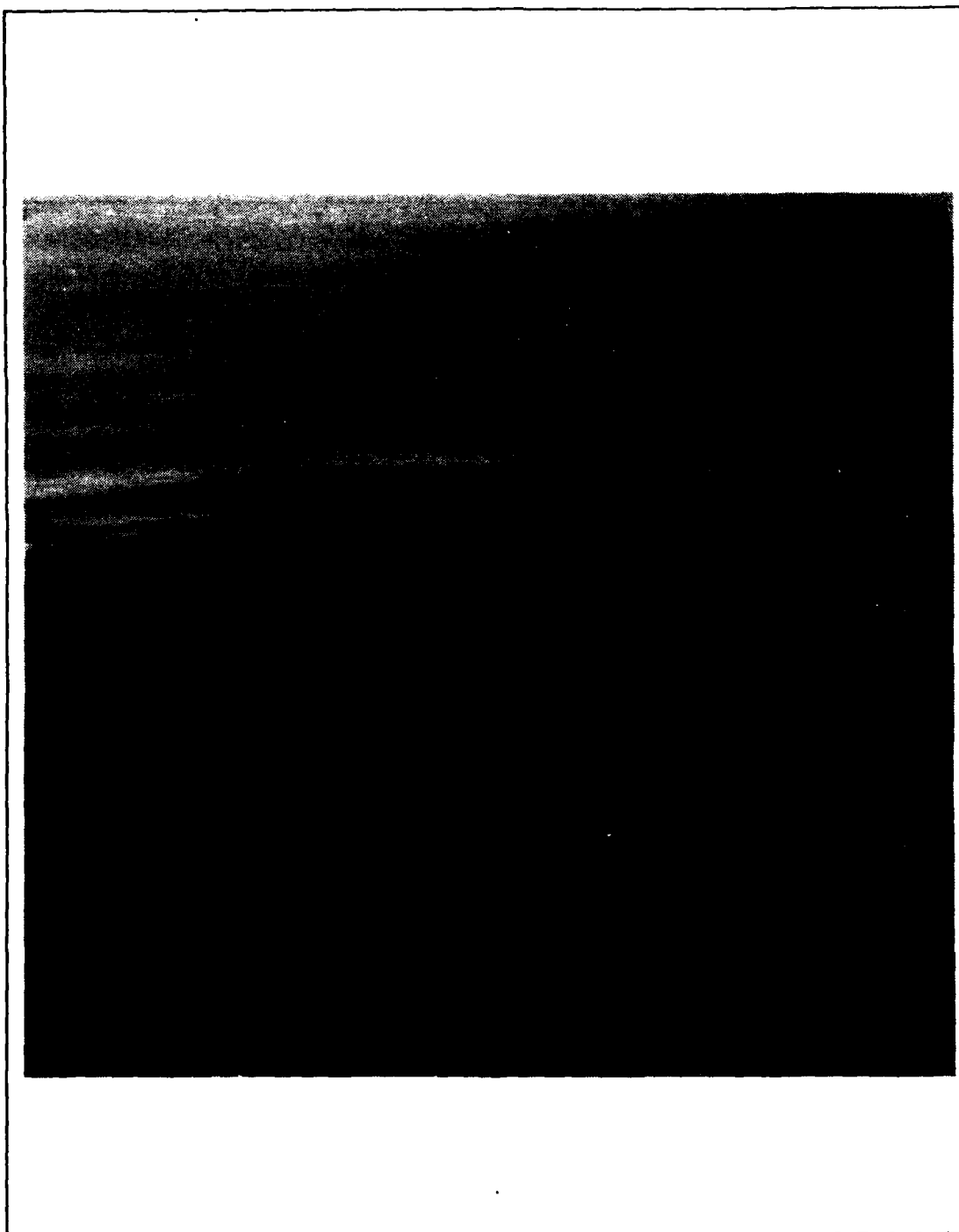


Figure 28. Photograph of Calm, "Patchy" Conditions: Observed during the afternoon of June 20, 1987.

Table 3. SKIN AND TWO METER TEMPERATURES: Observations of large variability between skin and two meter temperatures along Leg 21J. All temperatures in ° C.

TIME	T_{skin}	T_{2m}	ΔT
1428	11.52	11.18	0.34
1501	11.81	11.31	0.50
1516	13.00	11.26	1.74
1547	14.29	11.33	2.96
1606	16.23	11.52	4.71
1654	15.17	11.02	4.15
1744	13.13	10.59	2.54
1806	13.77	11.34	2.43
1910	13.42	11.50	1.92
1950	12.39	11.31	1.08
2028	12.28	11.24	1.04
2042	12.32	12.25	0.06

E. HEAT BUDGET CONSIDERATIONS

Short and long wave solar insolation were observed throughout the cruise using Eppley model PSP and PIR precision calibrated pyranometers. In what follows, all insolation variables were assumed to be uniform over the observed area, which seems reasonable for a short transect on a relatively calm day. This assumption is also in agreement with the results from CODE where the net surface heat fluxes were calculated at four separate meteorological buoys and were found to have a very high correlation [Lentz, 1987].

The primary variables in this problem are solar insolation (short and long wave), wind speed, air temperature and sea surface (skin) temperature. These variables are presented graphically in the panels of Figure 29, and in Table 4. The data begin at about sunrise and end about sunset (total elapsed time of about 18 hours). This interval represents the time period when short wave solar insolation is not zero. In an attempt to get the most representative values, the points that make up the plots are average values over one hour intervals. In Figure 29 the general pattern of short wave insolation is apparently starting at zero prior to sunrise and rising steadily to a maximum during the early afternoon. On the other hand, long wave insolation remains nearly constant over any given 24 hour period. Wind speed is generally less in the morning, increasing during the afternoon hours. Air temperature and skin temperature vary greatly and are

dependent upon all the variables above as well as upon each other and upon transient weather systems which can cause abrupt changes in each.

Murray [1987] showed how the Monin-Obukhov similarity theory could be used to calculate surface fluxes from SDAS data. He was able to calculate the scaled (bulk) parameters u , T , and Q , using a FORTRAN program PATFLUX provided by P. Guest at NPS based on the method of Large and Pond [1982].

A similar FORTRAN subroutine, BULKQ (also provided by P. Guest) was used to obtain bulk parameter values for the calculations below. The input variables for BULKQ are $U_{3.5}$, T_a , T_d , T_s , $CDN_{3.5}$, z_{0t} , and z_{0q} where

$U_{3.5}$ = true wind speed measured at 3.5 meters

T_a = air temperature measured at 3.5 meters

T_d = dew point temperature measured at 3.5 meters

T_s = skin temperature

$CDN_{3.5}$ = neutral drag coefficient at 3.5 meters

z_{0t} = temperature roughness scale

z_{0q} = humidity roughness scale

Typical open ocean values for z_{0t} and z_{0q} are 2×10^{-6} meters and a typical value for $CDN_{3.5}$ is 1.4×10^{-3} . The bulk parameters were calculated for each hourly point and are presented in Table 5.

The basic heat budget equation is

$$Q_0 = (1 - \alpha)Q_S + Q_L - Q_B - (Q_E + Q_H) \quad (Eq.1)$$

where

Q_0 = Net Radiative Heat Flux

Q_S = Solar Short Wave Radiation

Q_L = Solar Long Wave Radiation

Q_B = Long Wave Back Radiation from the Sea

Q_E = Evaporative/Latent Heat Flux

Q_H = Sensible Heat Flux

α = Albedo (reflected short wave radiation)

and horizontal advection has been neglected over such a short time scale. The units of Q are joules per second (watts) per square meter, or Wm^{-2} . The albedo varies with time

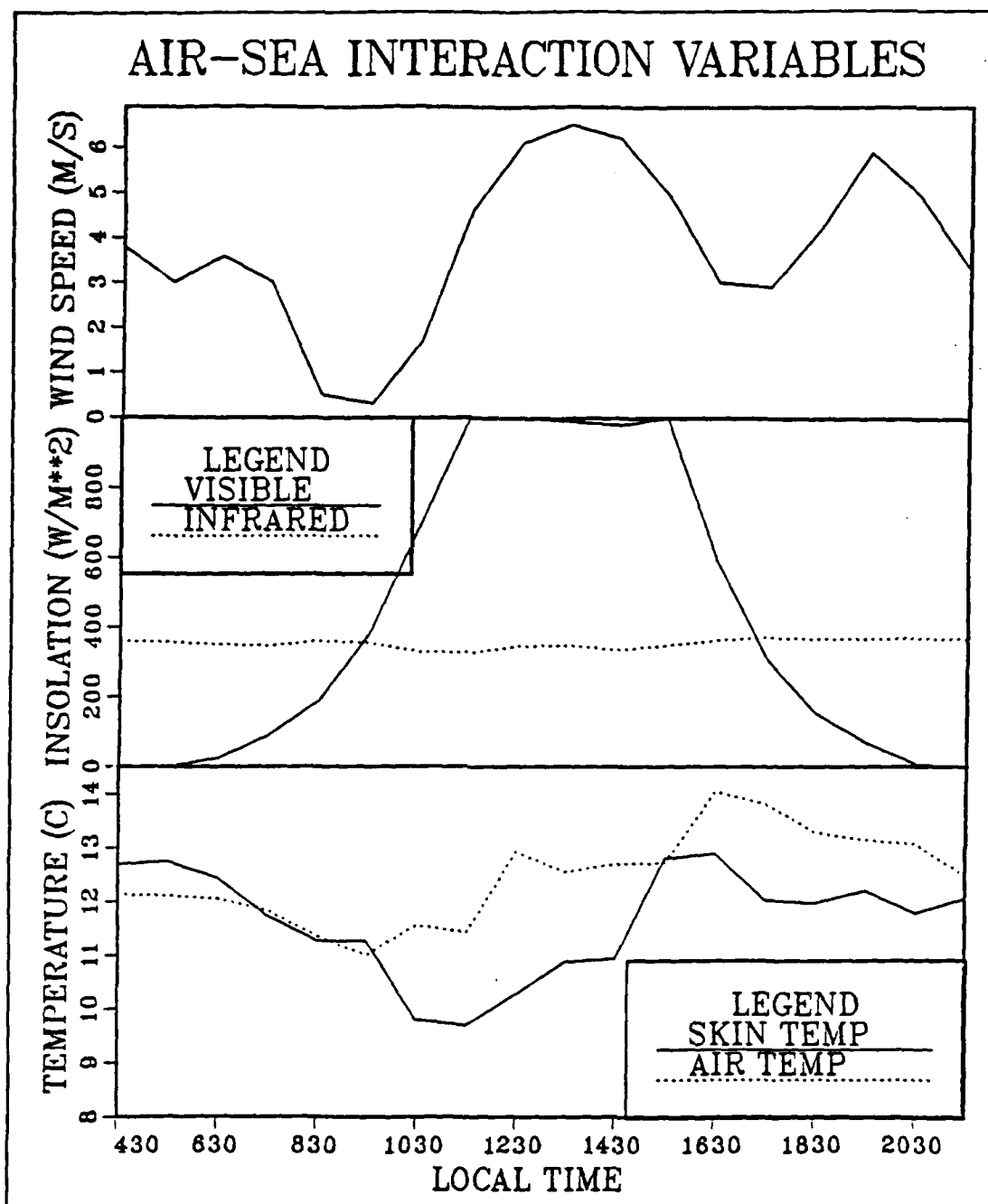


Figure 29. Plots of Primary Variables in the Air-Sea Interaction Problem: Taken along a track that includes Leg 21J on the 20th of June. Each point represents the variable's value averaged over one hour.

Table 4. HOURLY VALUES OF AIR-SEA INTERACTION VARIABLES

TIME	$U_{3.5}(ms^{-1})$	$T_a(^{\circ}C)$	$T_d(^{\circ}C)$	$T_s(^{\circ}C)$
0430	3.8	12.13	10.60	12.69
0530	3.0	12.11	10.58	12.74
0630	3.6	12.06	10.52	12.45
0730	3.0	11.84	10.46	11.75
0830	0.5	11.36	9.56	11.27
0930	0.3	11.00	8.27	11.27
1030	1.7	11.56	8.26	9.81
1130	4.6	11.42	8.20	9.70
1230	6.1	12.92	8.60	10.28
1330	6.5	12.55	9.17	10.88
1430	6.2	12.70	9.36	10.94
1530	4.9	12.72	9.36	12.79
1630	3.0	14.04	10.62	12.89
1730	2.9	13.81	10.62	12.02
1830	4.2	13.29	10.51	11.96
1930	5.9	13.14	10.44	12.19
2030	4.9	13.06	10.51	11.77
2130	3.8	12.48	10.62	12.03

of day, season, latitude and sea state. Gill [1982] states that within 40° of the equator, minimum albedo is below 0.1, with average values between 0.15 and 0.30. Due to the short time period involved and anomalous calm, clear weather conditions encountered, an estimated value of 0.1 is used for α . This is also consistent with the albedo of 0.07 used for heat budget studies in the CODE region near Point Arena [Lentz, 1987].

Looking at individual terms in equation 1:

- Values for Q_s and Q_L were measured directly using pyranometers mounted above the bridge of the R. V POINT SUR to avoid any obstruction. The data was monitored continuously, averaged every 30 seconds and stored in the SDAS.
- Q_B is estimated using Stephan's law for black body radiation which states that all bodies radiate energy at a rate proportional to the fourth power of their absolute temperature. The equation is

$$Q_B = \epsilon \sigma T_s^4 \quad (Eq.2)$$

where

T_s = absolute sea surface temperature ($^{\circ}K$)

$\sigma = 5.67 \times 10^{-8} W m^{-2} K^4$ (Stephan's constant)

ϵ = emissivity constant.

Table 5. CALCULATED BULK PARAMETERS u_* , T_* , and Q_* .

TIME	u_*	T_*	Q_*
0430	0.160	-.017	-.034
0530	0.128	-.019	-.036
0630	0.151	-.012	-.031
0730	0.125	0.002	-.020
0830	0.022	-.002	-.027
0930	0.016	-.011	-.054
1030	0.046	0.035	-.016
1130	0.183	0.046	-.020
1230	0.244	0.071	-.023
1330	0.264	0.045	-.025
1430	0.251	0.047	-.023
1530	0.204	-.003	-.053
1630	0.118	0.030	-.035
1730	0.107	0.045	-.020
1830	0.168	0.035	-.022
1930	0.242	0.025	-.027
2030	0.198	0.034	-.019
2130	0.156	0.012	-.022

Large *et al.* [1986] showed that the emissivity of the sea surface should be equal to one to properly account for reflected long wave radiation.

- The evaporative or latent heat flux is given by

$$Q_E = -\rho L_e u_* Q_* \quad (Eq.3)$$

where

ρ = density of sea water = 1.026 g cm^{-3}

L_e = latent heat of evaporation = 591 cal g^{-1}

u_* and Q_* are scaled velocity and humidity.

- The sensible heating is determined by

$$Q_H = -\rho C_p u_* T_* \quad (Eq.4)$$

where

C_p = specific heat of sea water = 1.0 cal g^{-1}

T_* = scaled temperature.

From the observations and calculations presented in Tables 4 and 5, the individual terms of the heat budget equation are calculated for each hour and are presented in Table 6 along with the observed values of short and long wave insolation. These values

are then summed over the period from the start of the heating day (about 0730 as seen by the first positive values of Q_0) to the time of maximum heating (approximately 1630) in order to determine the mean net radiative heat flux which was responsible for the observed temperature anomaly. Over this 10 hour period, the total heat added to the water can be determined by the equation

$$Q = \sum_{i=0}^{10} Q_{0i} \Delta t_i \quad (Eq.5)$$

which yields

$$Q = 5.16 \times 10^6 \text{ cal } m^{-2}.$$

The maximum difference between skin and two meters of $4.7^\circ C$ occurred at 1606 local time at about the 63 km point of Figure 16, about 10 hours into the heating day. The question is, can the measured/calculated value of Q raise the temperature of the upper ocean by $4.7^\circ C$ if it is trapped in a surface layer less than two meters deep? If turbulent mixing is confined to a very shallow mixed layer of depth H (the calm conditions encountered indicate that this assumption is valid), a volumetric approach to the heating problem can be used to determine an effective depth of heating. Starting with the formula

$$Q = \rho V \Delta T C_p \quad (Eq.6)$$

and solving for the volume, V

$$V = \frac{Q}{\rho \Delta T C_p} \quad (Eq.7)$$

If an area of one square meter is assumed, it follows that the depth, H , will be $H = V/A$. Substitution back into equation 7 yields

$$H = \frac{Q}{\rho A \Delta T C_p} \quad (Eq.8)$$

then using the values

$$Q = 5.16 \times 10^6 \text{ cal } m^{-2}$$

$$\rho = 1.026 \text{ g } cm^{-3}$$

$$\Delta T = 4.7^\circ C$$

Table 6. CALCULATED AND OBSERVED HEAT FLUX TERMS: Using equations 1-4. Units of Q are Wm^{-2} .

TIME	Q_S	Q_L	Q_B	Q_E	Q_H	Q_0
0430	0.0	359.5	378.2	13.8	23.4	-55.9
0530	0.4	356.9	378.5	11.7	19.8	-41.0
0630	23.8	349.7	377.0	11.9	20.1	-37.8
0730	88.7	347.2	373.3	6.4	-10.7	58.1
0830	187.6	360.2	370.8	1.5	2.6	154.2
0930	382.0	354.6	370.8	2.2	3.7	321.7
1030	691.1	330.4	363.2	1.9	-3.7	591.0
1130	999.0	328.0	362.7	9.3	-15.7	870.2
1230	999.0	345.7	365.7	14.2	-24.1	889.0
1330	990.0	349.0	368.8	16.7	-28.3	882.8
1430	980.0	335.9	369.1	14.7	-24.8	858.9
1530	999.0	349.4	378.8	27.4	2.6	839.7
1630	591.9	365.0	379.3	10.5	-17.7	525.7

$$C_p = 1.0 \text{ cal } g^{-1} ^\circ C^{-1}$$

$$A = 1.0 m^2$$

we see that $H = 1.07m = 107cm$. This effective depth is almost at the midway point between the skin and two meter sensors and indicates that it is possible for the 2 sensors to be completely uncorrelated when conditions such as those described above are encountered. The calculated solar heat flux could cause the observed ΔT on a very calm day when the surface mixed layer was ~ 1 meter deep.

A feature of Figure 16 which is not yet understood is the spatial patchiness at scales of about 10 kilometers, and this is recommended as a topic for further study.

IV. DISCUSSION

Throughout the CTZ pilot survey a broad, vast region of relatively cool, saline water was present off Point Arena. The first phase of the survey included several long transects which bisected the region of cool water completely, starting and finishing in the warm, oceanic waters which bounded the cool feature to the north and south. The survey track also extended far enough offshore so that the cool temperature signal was almost completely replaced by warmer oceanic waters and the higher salinity signal had completely disappeared. The dimensions of the feature were estimated from both cruise transects and satellite IR imagery as being ~ 100 kilometers in width with an offshore extension of ~ 300 kilometers. This pool of cool water appears to be periodically refreshed by narrow, cold filaments such as the one seen in the precruise satellite imagery (Figure 1) or by filament C which was investigated in the first and second phases. These narrow filaments appear to originate in the nearshore upwelling region near Point Arena.

During the first and second phases, filament C was observed in several transects as it moved offshore. There were several peculiarities noted as filament C evolved. Throughout the period when it was observed, the filament maintained a width from 10-30 kilometers. However, sometime during the weather delay between the end of phase two and the beginning of phase three, all surface traces of filament C disappeared while the broad, cool region remained intact.

Preliminary results from the survey cruises of the Coastal Transition Zone Experiment (Prof. S. Ramp, NPS; Prof. A. Huyer, Oregon State University; personal communication) indicate the presence of a continuous meandering upwelling jet off the central California coast from Cape Mendocino to at least Point Reyes. The cool pool of water at the surface off Point Arena (filament A) seems to be confined to the area on the nearshore side of this upwelling jet, which tends to meander far offshore in this region. The cool pool seems to be maintained despite intense summertime surface heating by the episodic injection of additional cold, salty water (filament C) from a nearshore upwelling center near Point Arena. Both filament C and a similar feature observed in the precruise imagery formed, moved offshore and disappeared in about six days. These smaller features seem to represent a delicate balance between the wind stress, solar insolation and mixing processes. Upwelling favorable winds bring the cold, salty water to the

surface near the coast, and are clearly necessary for filament formation, yet the wind stress also contributes to their mixing and eventual disappearance. The intense summer solar insolation would quickly mask the surface signature of the filaments without a continuous resupply of cold water from near the coast, and there is still the possibility that some of the cold water observed offshore comes from local upwelling. Clearly, the dynamics of these smaller filaments is complicated, and an accurate statement concerning their physics is beyond the scope of this paper. A detailed study of the vertical hydrographic sections, the acoustic doppler current data, and the wind stress time series from the NOAA buoys, together with this data set, is necessary to increase our understanding of the problem.

A very consistent characteristic of all the cold filaments was the distinct difference between the strengths of the temperature gradients at the north and south boundaries. The north wall gradient is always weaker than that observed at the south wall. These results also are in agreement with the observations of other CCS cold filaments [Flament *et al.*, 1985; Rienecker *et al.*, 1985]. During their 1982 survey as part of CODE, Kosro and Huyer [1985] observed a density compensating drop in salinity coincident with the south wall of a cold filament. Only one transect (leg IDC) indicated density compensation at the southern boundary which is consistent with the synopsis of Brink [1987], who observed that both cases have been seen in previous studies. Since the upwelled waters are cold and salty, and the surrounding waters are warm and fresh, the expectation is that the fronts will not be density compensated which is consistent with these results. During observations of filament C in phase one and two (Table 2), the gradient was strongest at a point along the filament (approximately 35 kilometers offshore), and not at the near-shore end. From the point of the strongest gradient, there was a steady decrease in gradient strength with increasing distance offshore. This was possibly the result of a disruption of the source waters corresponding to a relaxation of upwelling favorable winds [Flament *et al.*, 1985] during the period 20-21 June as observed from the R/V POINT SUR and NOAA bouy 46014 (39° 12' N, 124° 00' W). Filament A, the more permanent feature, was slightly different in that the gradients always weakened as offshore distance increased. All other characteristics noted above were the same.

Just what causes the filaments to move offshore is not known, but Figure 30 illustrates a few of the many possibilities which could explain all or part of the movement of cold filaments. Some of the suggested possibilities include interactions of the coastal waters with a meandering upwelling jet, effects of coastal convergence, advection due to

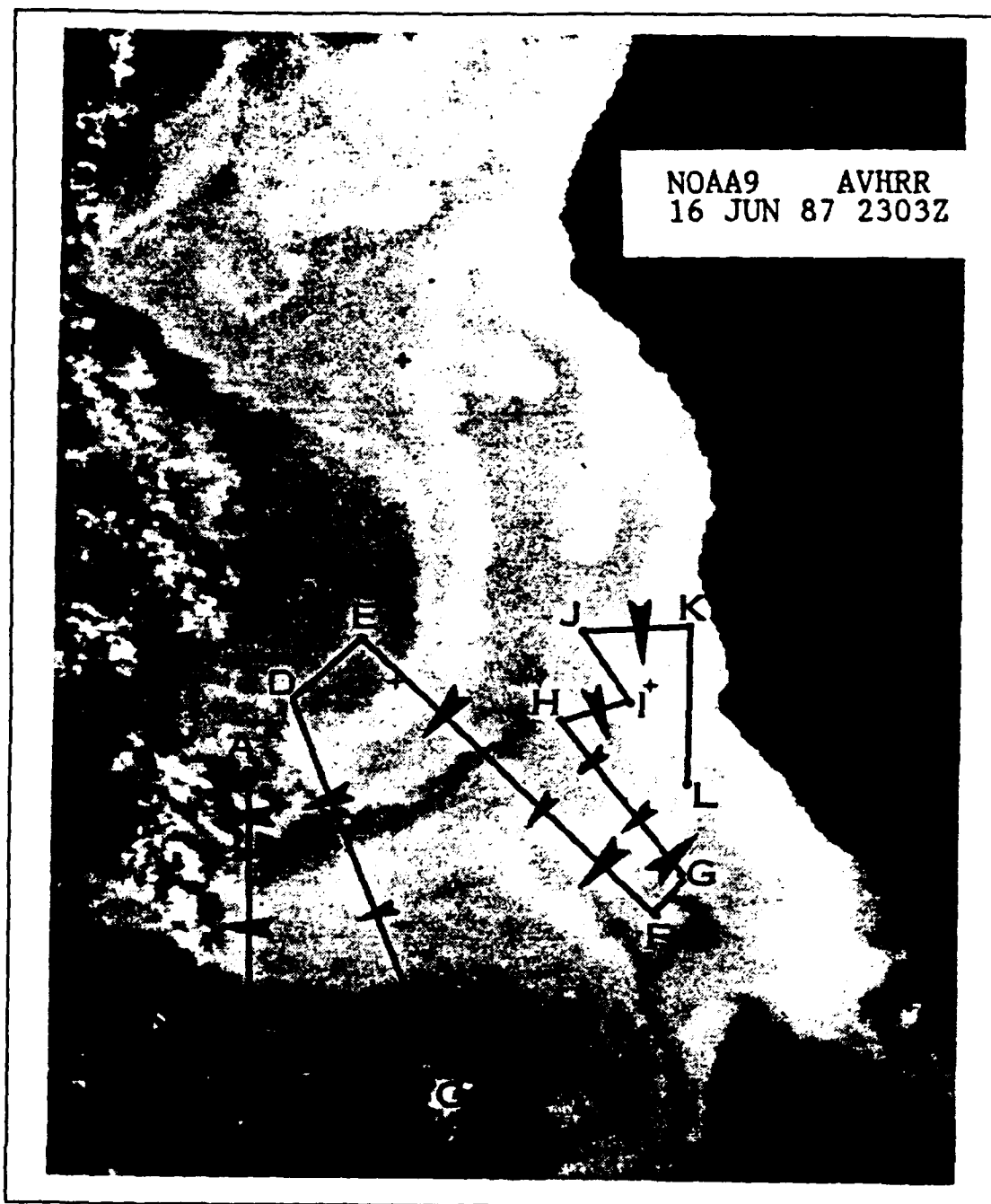


Figure 30. Superimposed Geostrophic Velocities: Calculated along each leg of phase one showing the complicated system of meanders and jets off Point Arena.

the interaction of eddies or effects of varying wind stress. The arrows along each of the transects represent the position and relative strength of the geostrophic surface currents relative to 500 decibars along each of the transects of phase one. The velocities were calculated from CTD data which was taken at 10 kilometer intervals along each leg. Nearshore, the flow was southerly to the north of Point Arena then it became westerly moving offshore as filament A. Near points F and G, the westward flow was associated with the beginning of filament C. To the north and further offshore, filament B was seen as it turned offshore after apparently originating near Cape Mendicino farther north. Between filaments A and B, there was an intrusion of oceanic water moving onshore. Presumably, this flow reversed later when the two filaments merged as observed in phase two. To the south, there was characteristic return flow [Flament *et al.*, 1985] of warmer oceanic water onshore. Near point G, there was also a shoreward flow, but it was not oceanic water and may have been due to a small eddy just to the south of filament C. Clearly, many processes are present in the total picture and at a given time, any or all of them may be important in filament formation, evolution and propagation.

It is also possible that coastal upwelling is not the only source of cold water for filaments. The dynamic height field for the second phase (Figure 31) indicates a very tight, narrow meander around filament A. The anticyclonic nature of the meander is conducive to divergence which could lead to local upwelling as a secondary source of cold water. Further investigation is required to determine whether there actually may be multiple sources of upwelled water. The ADCP data set may provide more information once it is fully analyzed.

Olivera *et al.* [1982] showed that, because density was mainly a function of temperature, maps of dynamic topography closely resemble satellite sea surface temperature images. This study generally confirms this result, however there were exceptions. The salinity signals vary greatly between different filaments. The boom probe sensor was designed to provide measurement of the same "skin temperature" seen by satellites. Under most conditions, this provided a very good representation of the underlying water characteristics, however, there were periods when light winds and surface heating combined to produce a distinct separation between the near-surface microlayer and depths as little as two meters. During these times, the sea surface temperature was clearly not representative of the underlying dynamic topography. This phenomenon seemed to be transient, forming in the afternoon during maximum solar insolation and mixes rapidly after short wave insolation drops off at the end of daylight hours.

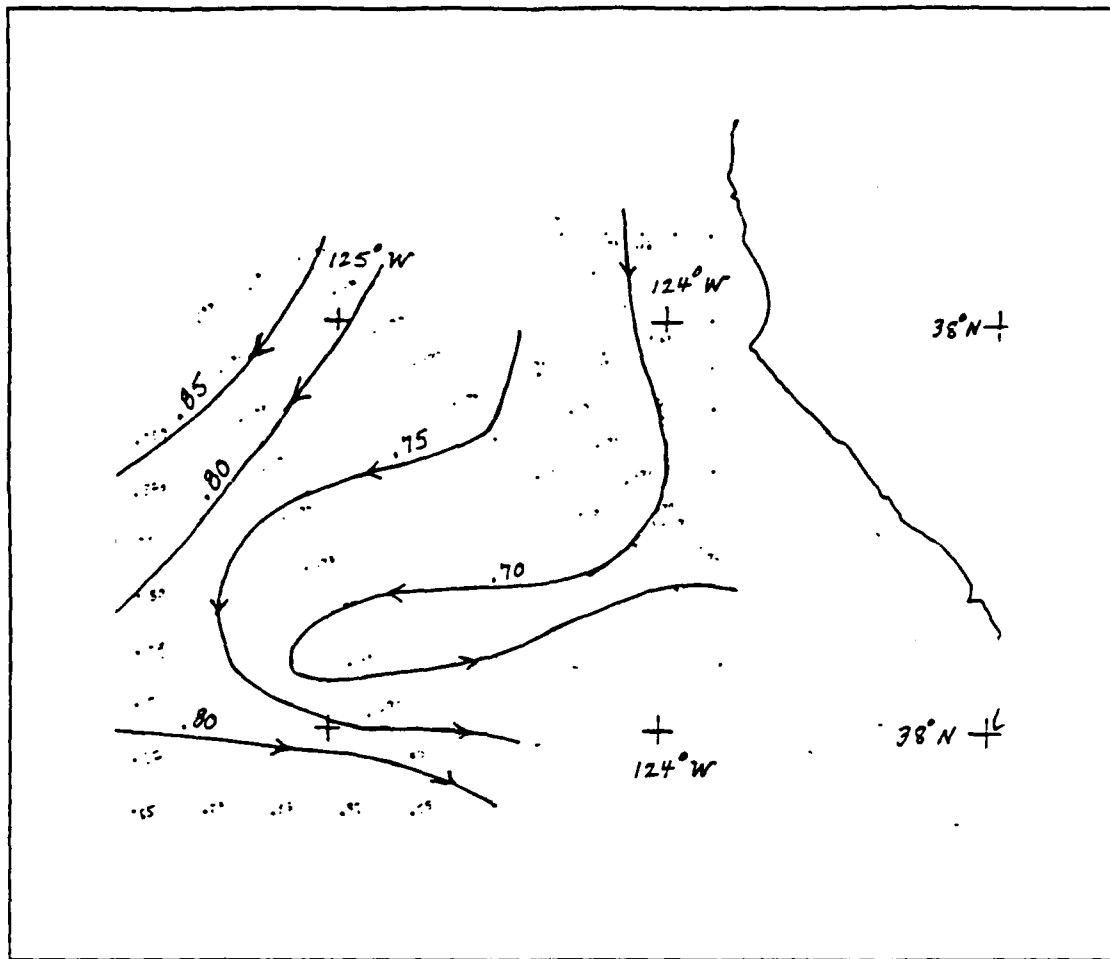


Figure 31. Dynamic Height Field Around Filament A: During phase one of the pilot survey, 15-19 June, 1987. Units are dynamic meters.

Regions of unordered, highly variable sea surface temperature off Point Arguello, California were also mapped by Brink *et al.* [1984]. They described them as superficial patches confined to a very thin surface layer and hypothesized their correlation to small eddies. These features may also be attributable to the manifestation of patchiness due to surface heating during periods of light, variable winds. During CODE, Davis [1985] used surface drifters to verify observations of a warm, high salinity, poleward moving pool of water being advected from the south near Point Arena. This flow reversal was associated with a wind relaxation event. Figure 16 illustrates that warm, high salinity surface water can be locally formed in a region dominated by cold, recently upwelled

water, at least on a transient basis. Without *in situ* verification, the presence of such a feature on satellite imagery cannot be interpreted as poleward advection of warm equatorial water.

V. CONCLUSIONS

Guided by infrared satellite imagery, high resolution mapping of the surface features of cold filaments was completed in a three phase survey off the California coast near Point Arena. Three distinct filaments were observed. Filament A was a persistent feature throughout the survey period which appeared to be a semi-permanent feature off Point Arena. It was a broad, ~ 100 kilometer wide feature extending ~ 300 kilometers offshore. Imbedded within filament A were two narrow, jet-like filaments. Filament B appeared to be the extension of a meander which originated to the north near Cape Mendicino. Filament C was rooted in the coastal upwelling center near Point Arena. Both of the narrow filaments maintained widths of order Rossby radius as they moved within filament A. Both of the narrow filaments eventually dissipated during the course of the survey and appear to be related to episodic events which serve to refresh and maintain filament A.

The surface signature of the north and south boundaries of the filaments was uniquely discernable by a strong horizontal temperature gradient. The gradient of the southern boundary was always significantly stronger than that of the northern boundary.

The complex patterns of the surface temperature fields seen in satellite imagery were usually representative of a surface mixed layer 20-50 meters deep. Only one anomalous period was observed where daytime insolation, in the absence of appreciable winds, created a surface microlayer significantly warmer than and uncorrelated with the underlying waters. Such features could be quite misleading in the interpretation of satellite sea surface temperature imagery.

As with previous studies, this survey provides information which for now, is only pertinent to the time and place that the data was taken. Before generalities can be made and model solutions can be tested, there is still much research that needs to be accomplished. Additional research in the following areas is recommended:

1. Complete processing of the CTD and ADCP data for comparison and verification of both horizontal and vertical structures. The need to provide the whole picture is obvious.
2. Investigate the spatial patchiness in surface heating which was observed during leg 2J1 via additional field and theoretical studies.

3. Continue with progressive research initiatives such as the upcoming CTZ to increase the CCS data bank and hopefully provide some answers to the many questions which still remain concerning the dynamics of upwelling filaments.
4. A continuous frustration throughout the program was the lack of a continuous time series of satellite imagery with which to correlate the cross-sections measured aboard ship. The scale of filaments A, B and C is such that they could be easily observed with the proposed microwave imaging systems, which can penetrate clouds and provide continuous remote sensing coverage. This thesis provides further evidence that such sensors should be placed in space at the earliest opportunity.
5. Investigate the acoustic implications of the strong surface fronts routinely seen in the California Current System. The strong surface temperature gradients measured during filament mapping indicate that these features form temperature fronts which are as strong as any seen in the world's oceans. The persistence of these filaments indicates that they may affect acoustic propagation along some regions of the California coast.

VI. LIST OF REFERENCES

- Bernstein, R. L., L. Breaker and R. Whritner, 1977: California Current eddy formation: ship, air and satellite results. *Science*, **195**, 353-395.
- Brink, K. H., D. W. Stuart, and J. C. Van Leer, 1984: Observations of the Coastal Upwelling Region near 34°30'N off California: Spring 1981. *J. Phys. Oceanogr.*, **14**, 378-391.
- Brink, K. H., 1987: Upwelling fronts: implications and unknowns. *S. Afr. J. Mar. Sci.*, **5**, 3-9.
- Davis, R. E., 1985: Drifter observations of coastal surface currents during CODE: the method and descriptive view. *J. Geophys. Res.*, **90**, 4741-4755.
- Flament, P., L. Armi, and L. Washburn, 1985: The evolving structure of an upwelling filament. *J. Geophys. Res.*, **90**, 11765-11778.
- Gill, A. E., 1982: *Atmosphere-Ocean Dynamics*, Academic Press, 652 pp.
- Huyer, A., 1983: Coastal upwelling in the California Current System. *Prog. Oceanogr.*, **12**, 259-283.
- Huyer, A. and P. M. Kosro, 1987: Mesoscale surveys over the shelf and slope in the upwelling region near Point Arena, California. *J. Geophys. Res.*, **92**, 1655-1682.
- Kelly, K. A., 1985: The influence of winds and topography on the sea surface temperature patterns over the northern California slope. *J. Geophys. Res.*, **90**, 11783-11798.
- Kosro, P. M. and A. Huyer, 1986: CTD and velocity surveys of seaward jets off northern California, July 1981 and 1982. *J. Geophys. Res.*, **91**, 7680-7690.

- Large, W. G. and S. Pond, 1982: Sensible and latent heat flux measurements over the ocean. *J. Phys. Oceanogr.*, **12**, 464-482.
- Large, W. G., J. C. McWilliams and P. P. Niiler, 1986: Upper ocean thermal response to strong autumnal forcing of the northeast Pacific. *J. Phys. Oceanogr.*, **16**, 1524-1550.
- Lentz, S. J., 1987: A heat budget for the northern California shelf during CODE 2. *J. Geophys. Res.*, **92**, 14491-14509.
- Murray, J. J., 1987: *An analysis of horizontal temperature gradients and heat content in the mixed layer and of the surface forcing during PATCHEX*. Masters Thesis, Naval Postgraduate School, Monterey, California, December 1987.
- Olivera, M., W. E. Gilbert, J. Fleischbein, A. Huyer, and R. Schramm, 1982: Hydrographic data from the first Coastal Ocean Dynamics Experiment, R/V WECOMA, Leg 7, July 1-14, 1981. *Ref. 82-8*, 170 pp., Sch. of Oceanogr., Oregon State Univ., Corvallis, Oregon, 1982.
- Rienecker, M. M., C. N. K. Mooers, D. E. Hagan, and A. R. Robinson, 1985: A coolanomaly off northern California: An investigation using IR imagery and *in situ* data. *J. Geophys. Res.*, **90**, 4807-4816.

VII. INITIAL DISTRIBUTION LIST

	No. Copies
1. Defense Technical Information Center Cameron Station Alexandria, VA 22304-6145	2
2. Library, Code 0142 Naval Postgraduate School Monterey, CA 93943-5002	2
3. Chairman (Code 68Co) Department of Oceanography Naval Postgraduate School Monterey, CA 93943-5000	1
4. Chairman (Code 63Rd) Department of Meteorology Naval Postgraduate School Monterey, CA 93943-5000	1
5. Prof. S. R. Ramp Department of Oceanography Naval Postgraduate School Monterey, CA 93943-5000	2
6. Prof. R. W. Garwood Department of Oceanography Naval Postgraduate School Monterey, CA 93943-5000	2
7. LCDR Richard L. Snow Executive Officer USS VREELAND (FF1068) FPO New York, NY 34093-1428	2
8. Director Naval Oceanography Division Naval Observatory 34th and Massachusetts Avenue NW Washington, DC 20390	1
9. Commanding Officer Naval Ocean Research and Development Activity NSTL Station Bay St. Louis, MS 39522	1

- | | | |
|-----|--|---|
| 10. | Commanding Officer
Naval Oceanographic Office
NSTL Station
Bay St. Louis, MS 39522 | 1 |
| 11. | Office of Naval Research (Code 1122PO)
800 N. Quincy Street
Arlington, VA 22217 | 1 |
| 12. | Chairman, Oceanography Department
U. S. Naval Academy
Annapolis, MD 21402 | 1 |
| 13. | Scientific Liaison Office
Office of Naval Research
Scripps Institution of Oceanography
La Jolla, CA 92037 | 1 |
| 14. | Dr. Alan Brandt
Office of Naval Research (Code 1122CS)
800 N. Quincy Street
Arlington, VA 22217 | 1 |
| 15. | Dr. Ken Brink
Woods Hole Oceanographic Institution
Woods Hole, MA 02543 | 1 |
| 16. | Dr. P. Michael Kosro
College of Oceanography
Oregon State University
Corvallis, OR 97331 | 1 |
| 17. | Dr. A. Jane Huyer
College of Oceanography
Oregon State University
Corvallis, OR 97331 | 1 |
| 18. | Dr. Libe Washburn
Department of Geological Sciences
University of Southern California
University Park
Los Angeles, CA 90089-0741 | 1 |
| 19. | Dr. Jim Simpson
Scripps Institution of Oceanography
University of California, San Diego
La Jolla, CA 92037 | 1 |